Caveolin-1 and -2 Interact with Connexin43 and Regulate Gap Junctional Intercellular Communication in Keratinocytes

Stéphanie Langlois,* Kyle N. Cowan,*† Qing Shao,* Bryce J. Cowan,‡ and Dale W. Laird*§

Departments of *Anatomy and Cell Biology, §Physiology and Pharmacology, and †Surgery, University of Western Ontario, London, ON N6A 5C1, Canada; and ‡Department of Dermatology and Skin Science, University of British Columbia, Vancouver, BC V5Z 4E8, Canada

Connexin43 (Cx43) has been reported to interact with caveolin (Cav)-1, but the role of this association and whether other members of the caveolin family bind Cx43 had yet to be established. In this study, we show that Cx43 coimmunoprecipitates and colocalizes with Cav-1 and Cav-2 in rat epidermal keratinocytes. The colocalization of Cx43 with Cav-1 was confirmed in keratinocytes from human epidermis in vivo. Our mutation and Far Western analyses revealed that the C-terminal tail of Cx43 is required for its association with Cavs and that the Cx43/Cav-1 interaction is direct. Our results indicate that newly synthesized Cx43 interacts with Cavs in the Golgi apparatus and that the Cx43/Cavs complex also exists at the plasma membrane in lipid rafts. Using overexpression and small interfering RNA approaches, we demonstrated that caveolins regulate gap junctional intercellular communication (GJIC) and that the presence of Cx43 in lipid raft domains may contribute to the mechanism modulating GJIC. Our results suggest that the Cx43/Cavs association occurs during exocytic transport, and they clearly indicate that caveolin regulates GJIC.

INTRODUCTION

Gap junctions are specialized intercellular membrane channels that allow direct transfer of molecules of <1000 Dalton to selectively pass from one cell to another (Sohl and Willecke, 2004; Laird, 2005). Gap junctional intercellular communication (GJIC) plays a critical role in the coordination of development, tissue function, and cell homeostasis (Segretain and Falk, 2004; Wei et al., 2004). Gap junction channels are composed of two hemichannels, termed connexons, each provided by one of the two contacting cells and each connexon is composed of six transmembrane proteins, called connexins (Cxs) (Laird, 2006). The large gene family encoding Cx comprises 21 members in human (Sohl and Willecke, 2004; Wei et al., 2004). Cx43 is the most abundant gap junction protein in a wide spectrum of tissues, including the epidermis (Kretz et al., 2004; Laird, 2006). Cx43 is most likely assembled into connexons in the trans-Golgi network and then traffics along microtubules to the plasma membrane where they diffuse laterally and aggregate into gap junction plaques (Saez et al., 2003; Martin and Evans, 2004; Segretain

and Falk, 2004; Laird, 2006; Lauf et al. 2002), although one report suggests that Cx43 containing vesicles may be directly targeted to adherens junctions adjacent to gap junctions (Shaw et al., 2007). The function of existing gap junction channels can be controlled by their opening and closing, whereas the regulation of their delivery, assembly, and removal constitutes additional mechanisms to control GJIC (Saez et al., 2003; Segretain and Falk, 2004; Laird, 2006). The extent of intercellular coupling is thus finely regulated by the control of connexin channels present at the plasma membrane, their functional state, and their permeability. All of these properties are determined by the constituent proteins of the connexon and their interaction with other protein partners and lipids (Cascio, 2005).

Various gap junction proteins are targeted to cholesterol-sphingolipid–rich membrane microdomains, called lipid rafts (Schubert et al., 2002; Lin et al., 2003, 2004; Barth et al., 2005; Laing et al., 2005; Locke et al., 2005), with several of these Cxs, including Cx43, having been shown to interact with caveolin (Cav)-1 (Lin et al., 2003, 2004; Schubert et al., 2002). Caveolins are cholesterol-binding integral membrane proteins that play a crucial role in the formation of caveolae, which are specialized invaginated raft domains (Parton et al., 2006). It has been recently identified that the Golgi complex is the site where newly assembled caveolar domains show up first, which are then directly transported and fuse to the plasma membrane (Tagawa et al., 2005). The formation and exit of caveolae from the Golgi complex is associated with caveolin oligomerization, acquisition of detergent insolubility, and association with cholesterol to form a mature caveolae-like exocytic structure (Parton et al., 2006; Parton and Simons, 2007). Although it is still unknown whether these proteins are transported to the plasma membrane in

caveolar carriers or via other exocytic pathways in a caveolin-dependent manner, the efficient plasma membrane delivery of the angiotensin II type 1 receptor, the insulin receptor, and transient receptor potential channel protein (TRPC1) has been reported to depend on Cav-1 (Brazer *et al.*, 2003; Cohen *et al.*, 2003; Wyse *et al.*, 2003; Parton and Simons, 2007). In addition, caveolins also function as scaffolding proteins capable of binding lipids and recruiting numerous signaling molecules into caveolae, as well as regulating their activity (Cohen *et al.*, 2004). Various channels have been shown to localize to and be functionally regulated by lipid rafts/caveolae (Lockwich *et al.*, 2000; Martens *et al.*, 2001; Yarbrough *et al.*, 2002; Barbuti *et al.*, 2004; Brainard *et al.*, 2005; Wang *et al.*, 2005; Balijepalli *et al.*, 2006). Cav-1 has been shown to modulate the activity of several channels (Trouet *et al.*, 1999, 2001; Toselli *et al.*, 2005), and more recently, it has been reported that Cav-1 regulates the function of the TRCP1 and the large conductance $Ca^{(2+)}$-activated K^+ channels by a direct physical interaction (Wang *et al.*, 2005; Kwiatek *et al.*, 2006; Remillard and Yuan, 2006).

Although Cx43 has been reported to target to lipid rafts and interact with Cav-1 (Schubert *et al.*, 2002), and it has been suggested that rafts might be involved in Cx trafficking (Locke *et al.*, 2005), the role of the Cx43/Cav-1 association, whether this interaction is direct or not, and whether other members of the caveolin family bind Cx43 had yet to be established. To investigate the role of caveolins in regulating Cx43 function, we chose to use keratinocytes, which endogenously express Cx43, Cav-1, and Cav-2. Cx43 and Cav-1 have both been associated with keratinocyte differentiation and transformation (Fitzgerald *et al.*, 1994; Sando *et al.*, 2003; Maass *et al.*, 2004), and skin carcinogenesis (Kamibayashi *et al.*, 1995; Capozza *et al.*, 2003). In this study, we mainly used a rat epidermal keratinocyte (REK) cell line that is phenotypically similar to basal keratinocytes in that they retain the ability to differentiate into organotypic epidermis (Maher *et al.*, 2005; Langlois *et al.*, 2007). In addition, Cx43 is found at the plasma membrane within gap junction plaques and within intracellular compartments in keratinocytes, thus allowing for the investigation of a possible role of caveolins in constitutive Cx43 trafficking and/or internalization. Using REKs, we have found that, in addition to Cav-1, Cx43 coimmunoprecipitates and colocalizes with Cav-2. The Cx43/Cav-1 colocalization was also observed in vivo in keratinocytes from human epidermis. Our results suggest that newly synthesized Cx43 and Cavs associate in the Golgi apparatus and most likely traffic together to the plasma membrane in lipid rafts. Mutation or deletion of Cx43 C-terminal tail (CT) inhibits its association with Cav-1 and -2, indicating that this domain is required for the Cx43/Cavs interaction. Our Far Western analysis confirmed the importance of the CT domain of Cx43 for its association with Cavs and indicates that Cx43CT can bind directly to Cav-1, suggesting that the Cx43/Cav-2 interaction might occur via Cav-1. Disruption of lipid rafts by using methyl-β-cyclodextrin (MβC) and diminution of Cav-1 and -2 expression by using small interfering RNA (siRNA), both reduced GJIC. These data were further confirmed by overexpressing Cav-1 in 293T cells, which express Cx43 but are deficient in Cavs, resulting in a significant enhancement of GJIC. Treatment with MβC and isolation of lipid rafts suggest that the presence of Cx43 in these specialized microdomains contributes to the mechanism regulating GJIC.

MATERIALS AND METHODS

Cell Culture

REKs and human embryonic kidney 293T were cultured in DMEM supplemented with 10% fetal bovine serum, 100 U/ml penicillin, 100 μg/ml streptomycin, and 2 mM glutamine. 293T cells were transfected using Metafectene transfection reagent (Biontex, Martinsried, Germany), as suggested by the manufacturer.

Engineering of the Cx43 DNA Constructs and Retroviral Infections

Generation of constructs containing cDNA for human Cx43-green fluorescent protein (GFP), G21R-GFP, G138R-GFP, G60S-GFP, and fs260-GFP within the adaptor protein (AP)2 replication-defective retroviral vector (Galipeau *et al.*, 1999) were described previously (Flenniken *et al.*, 2005; Gong *et al.*, 2006). In the cDNA encoding for Δ244-GFP Cx43 mutant, GFP was fused in frame to truncated Cx43 at amino acid 243 with the addition of seven amino acid linker sequence (GATCCACCGGTCGCCACC), and the DNA sequence was verified. Stable REK cell lines expressing Cx43-GFP, G21R-GFP, G138R-GFP, G60S-GFP, fs260-GFP, or Δ244-GFP cDNAs were generated by retroviral infection as described previously (Mao *et al.*, 2000; Qin *et al.*, 2002).

Engineering of the Cav-1 Small Interfering RNA Construct and Retroviral Infections

The coding region of rat Cav-1 gene was used for target gene sequence template. The siRNA sequence from Cav-1, ACCGCTTGCTGTCTAC-CATCTT (rat Cav-1 gene, GenBank accession no. BC078744, from 333 to 354), was selected using software from GenScript (Scotch Plains, NJ). GenScript synthesized the small DNA insert encoding a short hairpin targeting Cav-1 gene and cloned it into a pRNA-H1.1/Retro vector, which contains the human H1 promoter and the selection marker hygromycin. For simplicity, we refer to RNA interference (RNAi) reagents as siRNA. The Cav-1–targeted siRNA construct, together with an unrelated control siRNA vector, were used to make infectious viral supernatant as we described previously (Shao *et al.*, 2005). REKs were infected, cultured in selection medium containing 50 μg/ml hygromycin, and antibiotic-resistant cells were passed at least three times before further experimentation (Shao *et al.*, 2005).

Human Tissue Samples

Human facial skin samples were obtained after informed consent from patients attending the Vancouver General Hospital Skin Care Center (University of British Columbia, Vancouver, BC, Canada). During the reconstructive phase, after surgical removal of a cutaneous tumor, samples were taken from discarded normal tissue remote to the primary tumor site. Tissue collection was performed by Dr. Bryce J. Cowan in accordance with the ethical principles set forth in the Declaration of Helsinki and as instituted at the University of British Columbia. Samples were fixed in 10% neutral-buffered Formalin and subsequently embedded in paraffin.

Western Blotting

Wild-type, transfected, or infected cells were washed three times with cold phosphate-buffered saline (PBS) and scraped into 25 mM 2-(*N*-morpholino) ethanesulfonic acid, pH 6.5, and 0.15 M NaCl (MBS)-buffered saline containing 1 mM NaF, 1 mM Na_3VO_4, and protease inhibitor. The collected cells were sonicated and centrifuged to remove the debris from the lysates. Protein concentrations were determined using bicinchoninic acid assay (Pierce Biotechnology, Rockford IL). Proteins were resolved by SDS-polyacrylamide gel electrophoresis (PAGE), transferred to nitrocellulose membranes, and incubated in blocking buffer (LI-COR, Lincoln, NE) for 1 h, and then they were incubated with primary antibodies (β-actin, AC-15; Sigma-Aldrich. St. Louis, MO), early endosome marker EEA1 (ab2900; Abcam, Cambridge, MA), Cav-1 (clone polyclonal antibody [pAb]; BD Biosciences, San Jose, CA), Cav-2 (monoclonal antibody [mAb] clone 65, BD Transduction Laboratories, San Jose, CA), Cav-3 (clone 26; BD Biosciences), Cx43 (C6219; Sigma-Aldrich), or a mouse anti-Cx43NT (Goldberg *et al.*, 2002) overnight at 4°C. After three washes with Tris-buffered saline with Tween 20, infrared fluorescent-labeled secondary antibodies (IRDye 800 anti-rabbit or anti-mouse, Rockland Immunochemicals, Gilbertsville, PA; or Alexa-680 anti-rabbit or anti-mouse, Invitrogen, Carlsbad, CA) were incubated at room temperature for 1 h, and immunoblots were processed and quantified using the Odyssey infrared-imaging system (LI-COR).

Coimmunoprecipitation

Identical amounts of proteins from each lysate were incubated in immuno-precipitation (IP) lysis buffer (150 mM NaCl, 10 mM Tris-HCl, pH 7.4, 1 mM EDTA, 0.5% NP-40, and 1% Triton X-100) containing 1 mM NaF and 1 mM Na_3VO_4 overnight at 4°C in the presence of 2 μg/ml specific anti-Cav-1 (mAb clone 2297) or anti-Cav-2 (mAb clone 65) antibodies (BD Biosciences). The immune complexes were collected by incubating the mixtures with 30 μl (50% suspension) of protein A-Sepharose beads. Nonspecifically bound proteins

were removed by washing the beads three times in 1 ml of IP lysis buffer, and bound material was solubilized in 30 μl of twofold concentrated Laemmli sample buffer, boiled for 5 min, resolved by SDS-PAGE, and transferred to nitrocellulose membranes. Blots were probed with specific antibodies to detect Cx43, Cav-1, and Cav-2.

Immunofluorescence

To detect the different pools of caveolins, cells grown on glass coverslips were fixed with either 3.7% formaldehyde or 80% methanol:20% acetone (Bush *et al.*, 2006). 293T cells were fixed with 3.7% formaldehyde. Cells were permeabilized for 10 min in PBS with 0.2% bovine serum albumin (BSA) and 0.1% Triton X-100, and double-labeled for Cx43 and caveolins. Cells were labeled with either a polyclonal (1:200; Sigma-Aldrich) or a monoclonal anti-Cx43 antibody (clone P4G9 from the Fred Hutchinson Cancer Research Center Antibody Development Group, Seattle, WA). A fluorescein isothiocyanate (FITC)-conjugated anti-rabbit or anti-mouse IgG (1:200; Jackson ImmunoResearch Laboratories, West Grove, PA) was used as the secondary antibody for connexin labeling. For immunolocalization of caveolins, cells were labeled with a polyclonal anti-Cav-1 (1:50–1:100; pAb) or a monoclonal anti-Cav-2 antibody (1:50–1:100; clone 65). Texas Red-conjugated anti-rabbit or anti-mouse immunoglobulin G (IgG) (1:200; Jackson ImmunoResearch Laboratories) was used as the secondary antibody. For colabeling of Golgi markers, wild-type (WT) REKs and REKs overexpressing Cx43-GFP were labeled with either *trans*-Golgi network38 antibody (TGN38) (1:200; BD Biosciences Transduction Laboratories, Lexington, KY), or GPP130 (1:200; Covance, Berkeley, CA). FITC- and Texas Red-conjugated anti-rabbit or anti-mouse IgG were used as the secondary antibody. Cell cultures were then stained with Hoechst 33342 (1:1000; Invitrogen).

Human skin sections (5 μm in thickness) were deparaffinized in xylene, rehydrated in graded alcohols, and washed in PBS. Antigen retrieval was performed using Vector Antigen Unmasking Solution (Vector Laboratories) according to the manufacturer's protocol. To block nonspecific antibody binding, sections were incubated for 1 h at room temperature in PBS containing 3% BSA and 0.1% Triton X-100. Primary antibodies (Cx43 [P4G9], Cav-1 [1:100, pAb; BD Transduction Laboratories) were next applied to sections for 90 min at 37°C and diluted, where applicable, in PBS with 1% BSA, 0.1% Tween 20, and 0.01% SDS. Appropriate secondary antibodies diluted 1:100 in PBS with 1% BSA were then applied, conjugated to either Texas Red (Jackson ImmunoResearch Laboratories) or Alexa Fluor 488 (Invitrogen), and incubated for 1 h at room temperature. Hoechst 33342 (1:1000) was used as a nuclear stain. Sections were mounted with Vectashield mounting medium (Vector Laboratories, Burlingame, CA). In all cases, labeling was visualized with an LSM 510 META inverted confocal microscope (63× oil objective; Carl Zeiss, Jena, Germany).

Drug Treatments: Brefeldin A (BFA), MβC, and Cycloheximide (CHX)

Cells were treated for 6 h with 5 μg/ml BFA, for 1 h with 10 mM MβC, and for 6 h with 10 μg/ml CHX. BFA, MβC, and CHX were purchased from Sigma-Aldrich. After treatment, cells were fixed for immunofluorescence microscopy, lysed for immunoprecipitation and Western blotting, or used for Triton solubility and dye transfer assays.

Triton Solubility

Cells were washed three times with cold PBS. Triton solubility was assessed as described previously (Schubert *et al.*, 2002). Briefly, 600 μl of cold MBS containing 1% Triton X-100 plus 1 mM NaF, 1 mM Na$_3$VO$_4$, and proteases inhibitors was added to the cells. After a 30-min incubation without agitation on ice, the soluble fraction was collected. Six hundred microliters of 1% SDS was added to the 60-mm-diameter plate to dissolve the remaining Triton X-100–insoluble material. Equal volumes (25 μl) of the Triton X-100 soluble and insoluble fractions were separated by SDS-PAGE and subjected to immunoblotting as described above. EEA1 was used to verify the quality of the isolated fractions (Estall *et al.*, 2004).

Isolation of Lipid Rafts

Lipid rafts were isolated as described previously (Ostrom and Insel, 2006). Briefly, three 100-mm-diameter plates were washed three times with cold PBS, scraped into 750 μl of MBS containing 1% Triton X-100, and passed through a tight-fitting Dounce homogenizer (20 strokes). The sample was mixed with an equal volume of 90% sucrose (prepared in MBS lacking Triton X-100), transferred to a centrifuge tube, and overlaid with 4 ml of 35% sucrose, and overlaid with 4 ml of 5% sucrose (prepared in MBS lacking Triton X-100). The samples were centrifuged at 200,000 × *g* for 18 h in a Beckman SW41Ti rotor. Twelve fractions of 1 ml were collected starting at the top of the gradient, and aliquots of each fraction were subjected to SDS-PAGE and immunoblotting.

Cell Surface Biotinylation and Coimmunoprecipitations

Coimmunoprecipitations of biotinylated proteins were performed on the basis of a previously described protocol (Ray *et al.*, 1999). During the biotinylation procedure, all reagents and cultures were kept on ice. Cultures were washed three times in PBS, and then they were incubated in the same solution with EZ-link NHS-LC-biotin (0.5 mg/ml; Pierce Biotechnology) at 4°C for 20 min. Cells were washed once with PBS containing 100 mM glycine, and then they were incubated in glycine buffer for 15 min. Cells were washed again with glycine buffer and lysed either in IP buffer or in SDS lysis buffer (1% Triton X-100 and 0.1% SDS in PBS). Lysates were rocked for 1 h, and supernatants were either incubated overnight with 40 μl of neutravidin-agarose beads (Pierce Biotechnology) or first subjected to IP by using Cav-1 or Cav-2 antibodies. After IP, the beads were washed twice with coIP buffer and PBS, and then they were dried by aspiration. Immunoprecipitated proteins were collected in 2% SDS at 55°C for 5 min, diluted into IP buffer 5:1, and incubated with 40 μl of neutravidin-agarose beads overnight. Neutravidin beads were washed in IP buffer and PBS as described above, resuspended in Laemmli buffer, boiled for 5 min, resolved by SDS-PAGE, and transferred to nitrocellulose membranes. Blots were probed with specific antibodies to detect Cx43, Cav-1, and Cav-2.

Far Western Overlay Assay

Glutathione transferase (GST)-Cx43CT transformed into DH5α *Escherichia coli* was kindly provided by Dr. Lampe (Fred Hutchinson Cancer Research Center), and the GST fusion protein was expressed and purified using the Bulk GST purification module following the manufacturer's protocol (GE Healthcare, Little Chalfont, Buckinghamshire, United Kingdom). At the end of the purification steps, GST-Cx43CT was incubated with thrombin to obtain purified Cx43CT (amino acids 236–382).

Cav-1 was immunoprecipitated from three different sets of lysates from control or Cav-1–transfected 293T cells, immunoprecipitates were resolved by SDS-PAGE, and then they were transferred to nitrocellulose membrane. The membrane was blocked in 2% nonfat dry milk in PBS and incubated with Cx43CT (2 μg/ml in 2% dry nonfat milk/PBS) overnight at 4°C. The membrane was washed three times with PBS containing 0.05% Tween 20, and then it was incubated with anti-Cx43 antibody (1:500; Sigma-Aldrich), which recognizes the C-terminal domain of Cx43, for 2 h at room temperature. The membrane was washed three times, incubated with anti-rabbit antibody (Alexa 680 [red], 1:5000) for 1 h, and the immunoblot was processed using the Odyssey infrared-imaging system (LI-COR). To confirm that the band detected using Cx43CT corresponded to Cav-1, the same blot was probed with anti-Cav-1 antibody, washed, and incubated with anti-mouse antibody (IRDye 800 [green], 1:5000) as described above.

Dye Transfer

Confluent control or MβC-treated REKs or REKs infected with control or Cav-1–targeted siRNA constructs were used for microinjection. 293T cells transiently transfected with a control empty vector or with cDNA encoding Cav-1 monometric red fluorescent protein (mRFP) were also used. Random cells selected within control or MβC-treated WT and Cav-1 knockdown REKs were pressure microinjected. In the case of 293T cells, one cell expressing mRFP-tagged Cav-1 within a cluster of cells was pressure microinjected. In all cases, cells were microinjected with 1% Lucifer yellow in double-distilled H$_2$O (Invitrogen) until the cell was brightly fluorescent (<5 s) by using an Eppendorf FemtoJet automated pressure microinjector. After 1 min, the percentage of microinjected cells that transferred Lucifer yellow to at least one contacting cell was determined using a DM IRE2 inverted epifluorescent microscope (Leica Microsystems, Wetzlar, Germany). Digital images were collected with a charge-coupled device camera (Hamamatsu Photonics, Tokyo, Japan) by using OpenLab software (distributed by Quorum Technologies, Guelph, ON, Canada). At least 38 microinjections were performed for each experimental condition.

Statistics

All statistical data were analyzed using a one-way analysis of variance followed by a Tukey's test for significance, except for the data on the effect of MβC treatment on dye transfer in REKs and of Cav-1 overexpression on dye transfer in 293T cells, and the percentage of Cx43 present in raft and nonraft fractions in these cells. Because these data contained only two groups, they have been analyzed using two-tailed Student's *t* test.

RESULTS

Cx43 Coimmunoprecipitates with Cav-1 and Cav-2 in REKs

In addition to Cav-1, the caveolin gene family in mammals includes Cav-2 and -3. Cav-1 is expressed ubiquitously, although at various levels in different tissues. Cav-2 is coexpressed with Cav-1 in many cell types and tissues, whereas
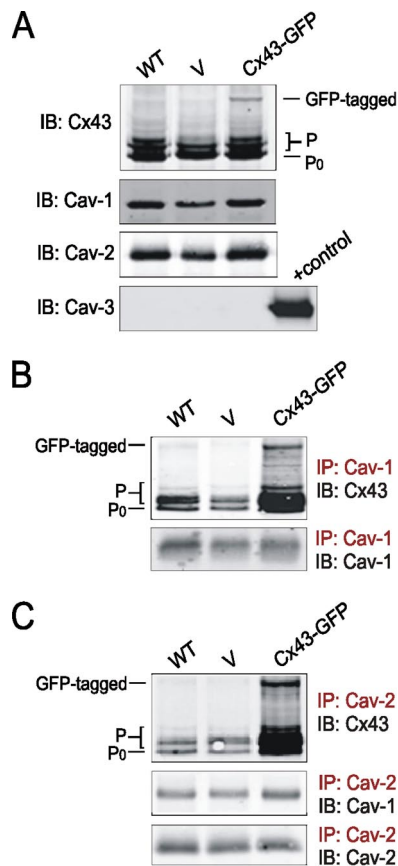
Figure 1. Cx43 coimmunoprecipitates with Cav-1 and Cav-2 in REKs. (A) WT REKs were infected with a vector encoding Cx43-GFP, or a control empty vector (V). Western blot showed that REKs express endogenous Cx43, Cav-1, and Cav-2, but not Cav-3 (positive control: muscle). (B) Both Cx43 (P_0 and P forms) and Cx43-GFP were found in Cav-1 immunoprecipitates. (C) Cx43 (P_0 and P forms) and Cx43-GFP, and Cav-1, coimmunoprecipitated with Cav-2. IP, immunoprecipitation; IB, immunoblotting.

Cav-3 is predominantly expressed in muscle cells (Williams and Lisanti, 2004). As shown in Figure 1A, WT REKs and REKs that express Cx43-GFP or the empty vector (V) express Cav-1 and -2, but not Cav-3. To examine the association of Cx43 with Cav-1 and its possible interaction with Cav-2, coimmunoprecipitation experiments were carried out. As reported previously (Schubert et al., 2002), the various phosphorylated species of endogenous Cx43 (P_0 and P), and Cx43-GFP, were found in Cav-1 immunoprecipitates (Figure 1B). When cell lysates were immunoprecipitated with antibodies directed against Cav-2, Cx43-GFP and Cx43 (P_0 and P) were also coimmunoprecipitated (Figure 1C). In keeping with the literature (Scherer et al., 1997; Scheiffele et al., 1998), Cav-1 was found associated with Cav-2 (Figure 1C). These results suggest that Cx43 interacts with Cav-1 and -2 as part of a multiprotein complex in REKs.

It is generally thought that the P_0 form of Cx43 assembles into connexons en route to the plasma membrane. Phosphorylation events that result in gel mobility shifts occur subsequent to delivery to the plasma membrane, and they are closely linked to accretion of connexons into gap junction plaques (Musil and Goodenough, 1991; Musil and Goodenough, 1993). The coimmunoprecipitation of the various phosphorylated species of Cx43 with Cavs suggests that

Cx43 en route to the cell surface interacts with Cav-1 and -2 in intracellular compartments and at the plasma membrane.

Cx43 Mainly Colocalizes with Cav-1 and Cav-2 in Intracellular Compartments of REKs

The next step was to identify in which cellular location the Cx43/Cavs interaction occurs. It is known that Cav-1 is the major structural component of caveolae and that it is also found in the Golgi complex of many cell types, whereas Cav-2 is often colocalized with Cav-1 (Williams and Lisanti, 2004). Given that no single staining condition is capable of detecting all the Cav-1 in a cell simultaneously (Bush et al., 2006), two different fixation methods were used. As shown in Figure 2, the localization of Cx43 was not dependent on the fixation method as in both cases (formaldehyde [A] or methanol:acetone [B] fixation) Cx43-GFP was found at the plasma membrane (Figure 2, A and B, top, green, arrowheads), and in intracellular compartments in a Golgi-like pattern (Figure 2, A and B, top, green, arrows). In formaldehyde-fixed cells, Cav-1 (Figure 2A, red, top, arrow) and Cav-2 (Figure 2A, red, middle, arrows) were mainly detected in intracellular compartments in a Golgi-like pattern. Overlay images revealed that Cx43-GFP is colocalized with Cav-1 and -2 (Figure 2A, yellow, top and middle, arrows) in intracellular compartments, most likely in the Golgi complex. As reported previously in Caco-2 cells (Breuza et al., 2002), colocalization of Cav-1 (Figure 2A, green, bottom) with Cav-2 (Figure 2A, red, bottom) was observed in a Golgi-like pattern (arrow) in WT REKs. Fixation of cells with methanol:acetone predominantly allowed the detection of Cav-1 (Figure 2B, red, top) and -2 (Figure 2B, red, middle) at the cell surface (Pol et al., 2005; Bush et al., 2006). Overlay images suggest that the majority of Cx43-GFP was not colocalized with Cav-1 and -2 at the plasma membrane and vice versa (Figure 2B, top and middle), but that few Cx43-GFP puncta were colocalized with Cavs (yellow, arrowheads) at the plasma membrane. However, in keeping with the literature (Scherer et al., 1996), the majority of Cav-1 (Figure 2B, red, bottom) and Cav-2 (Figure 2B, green, bottom) was colocalized at the cell surface (yellow, arrowheads). These data suggest that the Cx43/Cavs interaction mainly occurs in intracellular compartments, most likely in the Golgi complex, in REKs.

Cx43 colocalizes with Cav-1 in Keratinocytes of Human Epidermis

To examine whether the association of Cx43 with Cavs observed in REKs also occurs in vivo, Cx43 and Cav-1 were labeled in normal human epidermis. As reported previously (Masgrau-Peya et al., 1997; Tada and Hashimoto, 1997), Cx43 was weakly detected in the basal layer, but abundant in the spinosum layer and absent in the cornified layer (Figure 3, top, green). Specific Cav-1 staining was pronounced in basal and spinosum layers, and it was absent in the cornified layer (Figure 3, middle, red). The overlay image suggests that a pool of Cx43 was colocalized with Cav-1 in the spinosum and the basal layers (arrowheads) of human epidermis (Figure 3, bottom, yellow), suggesting that Cx43 may also interact with Cav-1 in human epidermal keratinocytes in vivo.

A Population of Cx43 Interacts with Cavs in the Golgi Apparatus

To characterize the Cx43/Cavs interaction, we first wanted to confirm that the colocalization of Cx43 with Cavs observed in the intracellular compartment of REKs corresponded to an association of these proteins in the Golgi apparatus. As shown in Figure 4A, Cx43, Cav-1, and -2 were
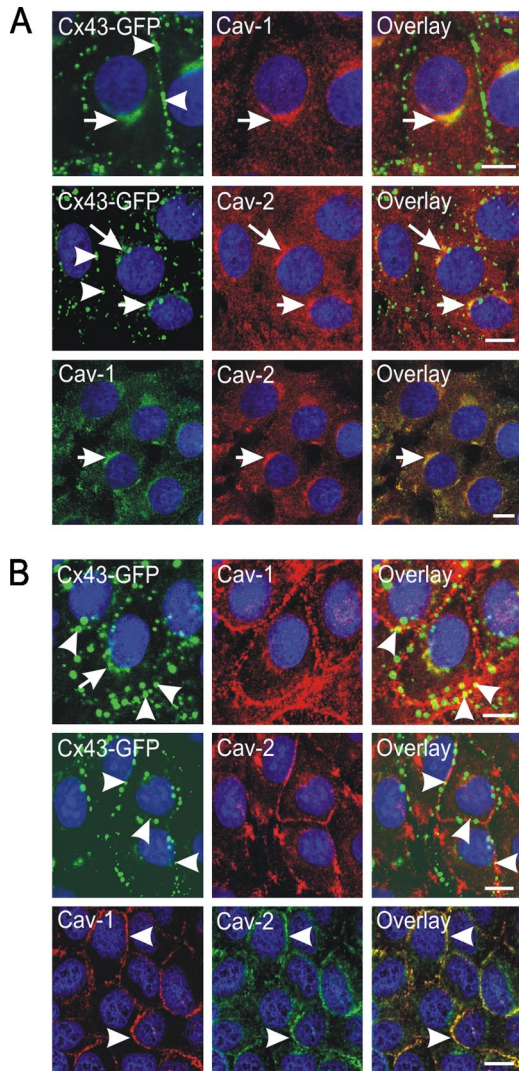
Figure 2. Cx43 mainly colocalizes with Cav-1 and -2 in intracellular compartments of REKs. (A) REKs or REKs overexpressing Cx43-GFP were fixed with formaldehyde and labeled with Cav-1 and -2. Confocal imaging of REKs overexpressing Cx43-GFP (A, green, top and middle) revealed Cx43 in gap junctions plaques at the cell surface (arrowheads) and in intracellular localization in a Golgi-like pattern (arrows). Cav-1 (red, top, arrow) and -2 (red, middle, arrows) were mainly detected in intracellular compartments in a Golgi-like pattern. Overlay images suggest that Cx43-GFP is colocalized (yellow, top and middle, arrows) with Cav-1 and -2 in the Golgi. Colocalization (yellow) of Cav-1 (green, bottom) with Cav-2 (red, bottom) was observed in intracellular compartments of REKs (arrow). (B) REKs or REKs overexpressing Cx43-GFP were fixed with methanol/acetone and labeled with Cav-1 and -2. Cx43-GFP (B, green, top and middle) was found in intracellular compartments (arrow) and at the plasma membrane (arrowheads), whereas Cav-1 (B, red, top) and -2 (B, red, middle) were mainly detected at the plasma membrane. Overlay images revealed that the majority of Cx43-GFP was not colocalized with Cav-1 and -2 at the plasma membrane. However, few Cx43-GFP plaques were colocalized with Cavs (yellow, arrowheads) at the plasma membrane. Colocalization (yellow, arrowheads) of Cav-1 (red, bottom) with Cav-2 (green, bottom) was observed at the plasma membrane of REKs. Blue, nuclei. Bars, 10 μm.

colocalized with resident constituents of the Golgi apparatus (TGN38 and GPP130), confirming their presence in this compartment. To verify that Cx43 colocalizes with Cavs in the
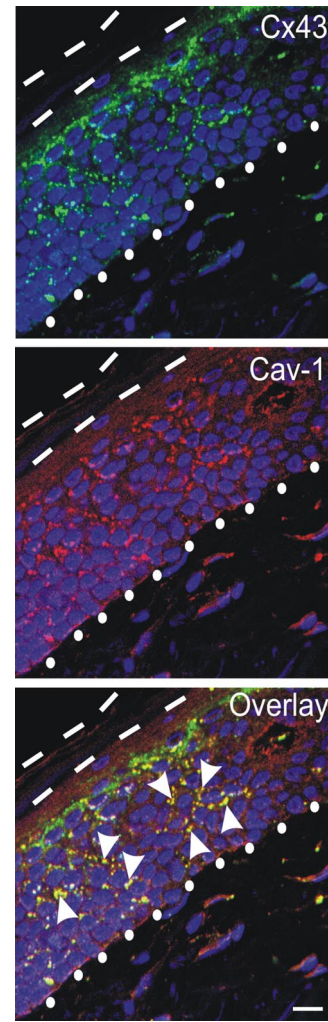
Figure 3. Cx43 colocalizes with Cav-1 in keratinocytes from human skin epidermis. Confocal imaging of human epidermis indicates that Cx43 (green, top) was detected in the vital layers (between dashed line and dotted line) and absent in the cornified layer (between dashed lines). Cav-1 staining (red, middle) was pronounced in basal and spinosum layers (between dashed line and dotted line), and it was absent in the cornified layer (between dashed lines). Overlay images suggest that Cx43 is colocalized with Cav-1 in the vital layers of human epidermis (yellow, arrowheads, bottom). Blue, nuclei. Bar, 10 μm.

Golgi, REKs overexpressing Cx43-GFP were treated with BFA, which disrupts the Golgi assembly and redistributes proteins to the endoplasmic reticulum, and labeled for Cav-1 and -2. In keeping with the literature (Musil and Goodenough, 1993; Laird *et al.*, 1995; Thomas *et al.*, 2005), treatment with BFA blocked the trafficking of Cx43-GFP to the cell surface (Figure 4B, green, top and middle), as opposed to untreated cells in which Cx43-GFP was present within gap junctions plaques at the plasma membrane (Figure 4B, green, inset, top). As reported previously (Laird *et al.*, 1995), treatment with BFA also prevented the phosphorylation of the P_0 form of Cx43 to the phosphorylated (P) species (Figure 4C). Similar to Cx43-GFP, the staining of Cav-1 (Figure 4B, red, top) and Cav-2 (Figure 4B, red, middle) in the Golgi complex were lost after BFA treatment, whereas their expression levels remained constant (Figure 4C). Both Cx43-GFP and Cavs were thus dispersed throughout the cell after
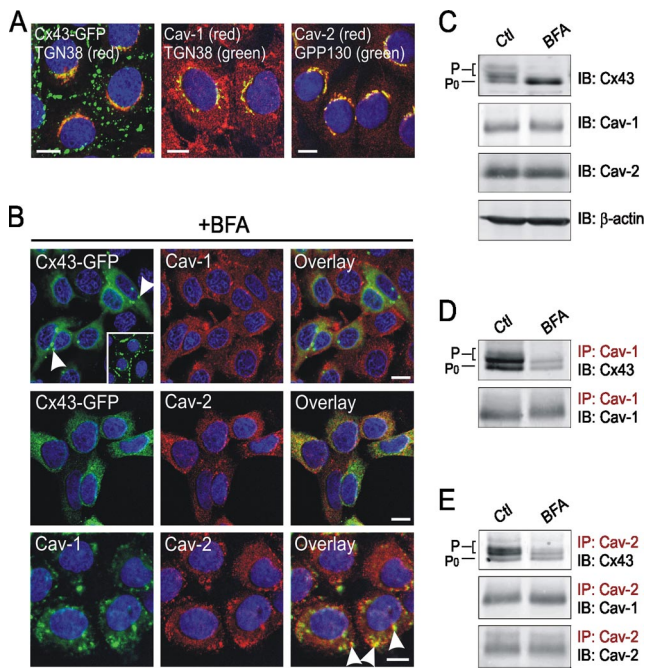
Figure 4. Cx43 colocalizes with Cavs in the Golgi apparatus. (A) REKs overexpressing Cx43-GFP were labeled with TGN38 (red, left), and REKs were colabeled for Cav-1 (red, middle) and TGN38 (green) or with Cav-2 (red, right) and GPP130 (green). Overlay images show that Cx43-GFP, Cav-1, and Cav-2 were colocalized (yellow) with the resident Golgi proteins. REKs or REKs overexpressing Cx43-GFP were treated with BFA for 6 h before their fixation with formaldehyde and labeling with Cav-1 and -2. (B) Treatment with BFA resulted in a loss of most Cx43-GFP (green, top and middle) at gap junction plaques (arrowheads), compared with untreated cells (green, inset, top). Golgi localization of Cx43-GFP (green, top and middle), Cav-1 and -2 (red, top and middle) was lost in BFA-treated cells. Colocalization of Cav-1 (green, bottom) with -2 (red, bottom) in the Golgi was lost in REKs. Blue, nuclei. Bar, 10 μm. (C) Lysates from untreated and BFA-treated REKs were subjected to Western blot. BFA treatment dramatically reduced the P species of Cx43. β-Actin was used as a loading control. Treatment with BFA reduced the amount of Cx43 found in Cav-1 (D) and Cav-2 (E) immunoprecipitates, without affecting the amount of Cav-1 coimmunoprecipitating with Cav-2 (E). IP, immunoprecipitation; IB, immunoblotting.

treatment with BFA. However, Cav-1 and -2 remained colocalized in intracellular compartments (Figure 4B, yellow, bottom, arrowheads), most likely in lipid bodies (Fujimoto *et al.*, 2001; Pol *et al.*, 2004). Although faint bands corresponding to the Cx43 phosphorylated species (P) could be detected in the Cavs immunoprecipitates after BFA treatment in some experiments, probably reflecting treatment efficiency, the amount of Cx43 that coimmunoprecipitated with Cav-1 (Figure 4D) and Cav-2 (Figure 4E) was consistently reduced. In accordance with our colocalization data, the amount of Cav-1 associated with Cav-2 was not affected by BFA (Figure 4E). Together, these results confirm that a population of Cx43 interacts with Cavs in the Golgi apparatus.

Newly Synthesized Cx43 and Cavs Colocalize in the Golgi Apparatus

Golgi-associated caveolins could be either en route to the cell surface from its site of synthesis in the ER, or having arrived via a recycling pathway (Nichols, 2002; Pol *et al.*, 2005). To discriminate between these two possible trafficking path-
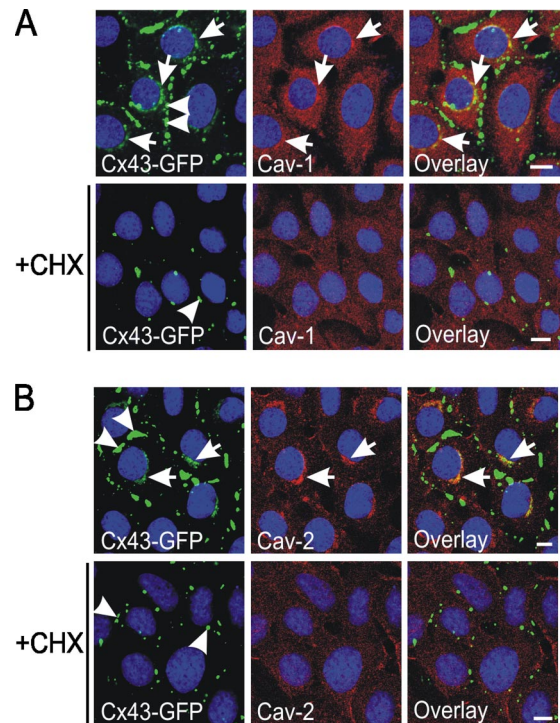

Figure 5. Newly synthesized Cx43 and Cavs colocalize in the Golgi apparatus. REKs overexpressing Cx43-GFP were treated with CHX for 6 h before their fixation with formaldehyde and labeling with Cav-1 (A) and -2 (B). Treatment with CHX resulted in a loss of Cx43-GFP in gap junction plaques (A and B, green, arrowheads). It also resulted in a loss of the intracellular pools of Cx43-GFP (A and B, green, arrows), Cav-1 (A, red, arrows), and Cav-2 (B, red, arrows) in the Golgi apparatus. Blue, nuclei. Bars, 10 μm.

ways, CHX was used to inhibit protein synthesis leading to a loss of Golgi localization of newly synthesized proteins without affecting the cycling of proteins from the plasma membrane to the Golgi complex. After treatment with CHX, REKs overexpressing Cx43-GFP were fixed with formaldehyde to detect the Golgi-associated pool of caveolins and labeled for Cav-1 and -2. Inhibition of protein synthesis resulted in a loss of Cx43-GFP in the Golgi apparatus (arrows), and a reduction in cell surface gap junction plaques (arrowheads) (Figure 5, A and B, green). In accordance with previous reports (Nichols, 2002; Pol *et al.*, 2005; Tagawa *et al.*, 2005), treatment with CHX also resulted in disappearance of Cav-1 (Figure 5A, red) and -2 (Figure 5B, red) in the Golgi (arrows). Overlay images indicate that, as opposed to control cells (Figure 5, A and B, top, yellow, arrows), the colocalization of Cav-1 and -2 with Cx43-GFP in the Golgi was lost after treatment with CHX (Figure 5, A and B, bottom). Although these results cannot rule out a possible role of internalization, it indicates that at least a pool of Cx43 and Cavs found colocalized in the Golgi apparatus correspond to newly synthesized proteins.

A Population of Cx43 Targets and Interacts with Cavs at the Plasma Membrane in Lipid Rafts

It has been recently identified that the Golgi complex is the site where newly assembled caveolar domains occur first (Tagawa *et al.*, 2005). Newly synthesized caveolin in the Golgi complex is mobile and not associated with detergent-resistant membranes or lipid rafts. At some point in the biosynthetic pathway, caveolin associates with lipid rafts,
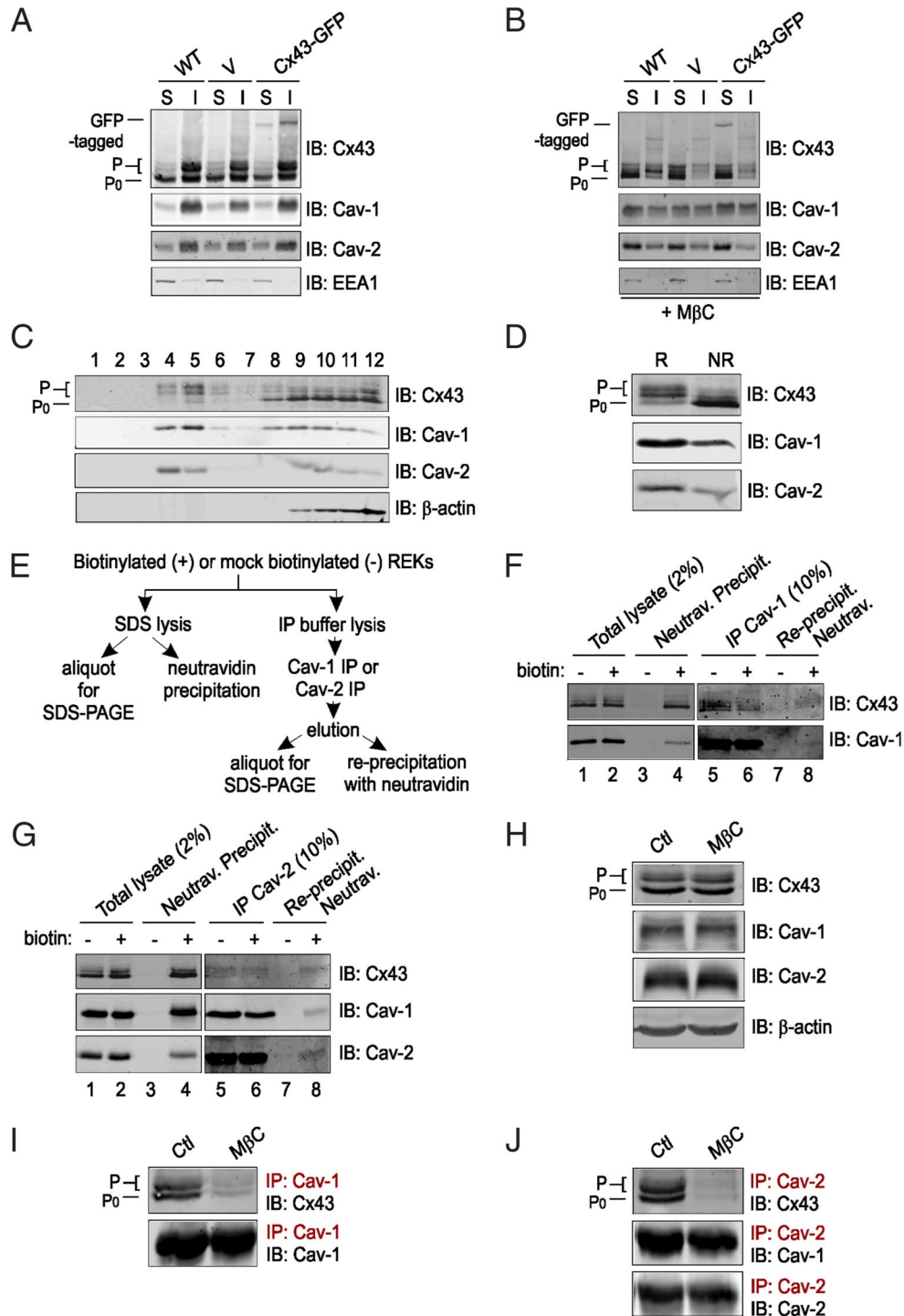
Figure 6. A population of Cx43 interacts with Cavs at the plasma membrane in lipid rafts. WT REKs or REKs infected with Cx43-GFP, or the control empty vector (V), were treated with 10 mM MβC for 1 h. Untreated (A) and treated cells (B) were lysed in 1% Triton X-100 to obtain insoluble (I) and soluble (S) fractions, which were analyzed by Western blotting. EEA1 was used as a fractionation control. Note that Cx43, Cav-1, and Cav-2 were mainly found in the Triton-insoluble fractions (I), but that they were translocated to Triton-soluble fractions (S) after MβC treatment. (C) WT REKs were subjected to sucrose density gradient centrifugation. Twelve fractions were collected and analyzed by Western blot. Note that the fractions 4–6 (raft) are enriched in the P forms of Cx43, whereas the fractions 8–12 (nonraft) are enriched in the P_0 form. (D) Fractions 4–6 (R) and fractions 8–12 (NR) were pooled and equal amounts of proteins were subjected to Western blotting. REKs were biotinylated (+), or subjected to mock biotinylation (−), and then subjected to coimmunoprecipitations by using Cav-1 and Cav-2 antibodies, as presented in the scheme (E). SDS extracts were collected, and an aliquot (2%) was analyzed by Western blot (F and G, lanes 1 and 2); the remainder of the lysates underwent neutravidin precipitation before SDS-PAGE (F and G, lanes 3 and 4). Cx43, Cav-1, and Cav-2 were recovered when REKs were treated with biotin (F and G, lane 4), but not when biotin was omitted (F and G, lane 3). The Cx43/Cav-1 and Cx43/Cav-2 complexes were recovered by anti-Cav-1 (F, lanes 5 and 6) and anti-Cav-2 IP (G, lanes 5 and 6), eluted from the antibodies, and aliquots (10%) were analyzed directly. The remainder of the immunoprecipitates underwent neutravidin precipitations followed by SDS-PAGE (F and G, lanes 7 and 8). Biotinylated Cx43 was

becomes detergent insoluble, and is organized into higher order oligomers that are characteristic of the surface pool of this protein (Parton and Simons, 2007). To determine whether Cx43 is present in lipid rafts, we first enriched these detergent-resistant membranes on the basis of their resistance to solubilization by mild nonionic detergents at 4°C (Williams and Lisanti, 2004). In accordance with previous reports (Song *et al.*, 1997; Galbiati *et al.*, 1998; Parolini *et al.*, 1999; Schubert *et al.*, 2002; Mograbi *et al.*, 2003; Barth *et al.*, 2005), the phosphorylated species (P) of Cx43, and Cav-1 and -2, were mainly Triton insoluble, whereas the P_0 form of Cx43 was present in both Triton-soluble and -insoluble fractions (Figure 6A). Similar to the behavior of endogenous Cx43, Cx43-GFP was found to be predominantly Triton insoluble (Figure 6A). Next, we used a common method for confirming raft association consisting of disrupting raft integrity or lipid content from the plasma membrane by using the cholesterol-depleting agent MβC (Simons and Ehehalt, 2002; Giocondi *et al.*, 2004). As expected, treatment with MβC resulted in a translocation of Cav-1 and -2 into the Triton-soluble fractions (Figure 6B). Endogenous Cx43 and overexpressed Cx43-GFP also became mainly Triton soluble after treatment with MβC (Figure 6B), suggesting that a population of Cx43 is targeted to lipid rafts domains with Cavs in REKs.

To further assess the presence of Cx43 in lipid rafts, these domains were then isolated using an established equilibrium sucrose density gradient system (Lisanti *et al.*, 1994; Scherer *et al.*, 1994; Ostrom and Insel, 2006), and the presence of Cx43, Cav-1, and Cav-2 was determined by Western blotting (Figure 6C). The presence of Cx43 and Cavs in raft (R) and nonraft fractions (NR) was also assessed in pooled fractions 4–6 (R) and in pooled fractions 8–12 (NR) loaded at equal amount of proteins. As anticipated, a population of Cav-1 and -2 was found in raft-enriched membranes (Figure 6C, fractions 4–6, and D), which exclude >99.95% of total cellular proteins and markers for nonraft plasma membrane, Golgi apparatus, lysosomes, and endoplasmic reticulum (retained in fractions 8–12) (Sargiacomo *et al.*, 1993; Lisanti *et al.*, 1994; Scherer *et al.*, 1994). A population of Cav-1 and -2 was also found in the nonraft membrane fractions (Figure 6C, fractions 8–12, and D), which most likely represent the detergent-soluble newly synthesized caveolins (Pol *et al.*, 2005). As shown in other cell types (Schubert *et al.*, 2002; Lin *et al.*, 2003; Mograbi *et al.*, 2003; Barth *et al.*, 2005) and in keeping with our Triton solubility data (Figure 6A), the P_0 form of Cx43 was detected in rafts, but these fractions were mainly enriched in its phosphorylated species (P) (Figure 6C, fractions 4–6, and D). Although the nonraft fractions mainly contained the P_0 form of Cx43, its phosphorylated species were also detected (Figure 6C, fractions 8–12, and D). These data clearly show that a population of Cx43 is targeted with Cavs to lipid rafts in REKs.

Because our colocalization data suggest that only a small population of Cx43 and Cavs are associated at the cell surface, we wanted to confirm the presence of the Cx43/Cavs complex at the plasma membrane; thus, we performed bioti-

nylation/coimmunoprecipitation experiments (Figure 6E). Extracellular proteins were labeled with biotin on ice to limit intracellular transport to, and internalization from, the cell surface. After biotin treatment, the various phosphorylated species of Cx43 (P and P_0) were recovered with neutravidin, and Cav-1 and Cav-2 (Figure 6, F and G, lane 4), indicating their presence at the plasma membrane. No Cx43 or Cavs were recovered when biotin was omitted as a control (Figure 6, F and G, lane 3). In parallel, the Cx43/Cavs complexes were recovered by Cav-1 and Cav-2 immunoprecipitations to determine whether any of the Cx43 bound to Cavs had been biotinylated. When the Cx43 bound to Cav-1 (Figure 6F, lanes 5 and 6), and to Cav-2 (Figure 6G, lanes 5 and 6), was eluted and reprecipitated with neutravidin, Cx43 was recovered from biotin-treated REKs (Figure 6, F and G, top, lane 8), but not from the untreated cells (Figure 6, F and G, top, lane 7). In addition, when the proteins bound to Cav-2 have been eluted and reprecipitated with neutravidin, Cav-1 was also recovered (Fig, 6G, middle, lane 8) confirming the association of Cav-1 with Cav-2 at the plasma membrane. Although the amounts were low, biotinylated Cav-1 and Cav-2 were recovered in their respective immunoprecipitates (Figure 6, F and G, bottom, lane 8). To further assess whether the Cx43/Cavs association detected at the plasma membrane occurs in lipid rafts, REKs were treated with MβC, and coimmunoprecipitation experiments were performed. Although there were variations in the extent of dissociation, overall the treatment with MβC resulted in the reduction of the association of Cx43 with Cav-1 (Figure 6I) and Cav-2 (Figure 6J) without significantly altering the expression levels of these proteins (Figure 6H). However, treatment with MβC did not affect the extent of the association between Cav-1 and -2 (Figure 6J). Together, these results indicate a population of Cx43 is targeted to lipid rafts and interacts with Cavs in these specialized microdomains at the plasma membrane.

The C-terminal Tail of Cx43 Is Required for Its Association with Cavs

It has been reported previously that Cx43 interacts with the caveolin-scaffolding and the C-terminal domains of Cav-1 (Schubert *et al.*, 2002). However, the domain(s) of Cx43 involved in this association and in its newly described interaction with Cav-2 remained to be determined. To identify which part of Cx43 molecule is involved in its interaction with Cavs, we stably overexpressed five GFP-tagged Cx43 mutants (G21R, G138R, G60S, fs260, and Δ244) in REKs, and WT Cx43-GFP (Figure 7A). These mutants were specifically chosen because they each represent mutations or truncations in distinct Cx43 domains (Figure 7A). Although some of these Cx43 mutant motifs were unlikely to be topologically available to interact directly with Cavs embedded in the plasma membrane, they were still assessed for their ability to associate with Cavs as the interaction could be indirect and occurring through protein complexes that could possibly involve the transmembrane and/or extracellular domains of the Cx43 molecule. The G21R, G138R, and fs260 mutants are linked to oculodentodigital dysplasia (ODDD), which is an autosomal dominant disorder caused by mutations in the gap junction α 1 gene (*GJA1*) encoding Cx43 (Paznekas *et al.*, 2003; van Steensel *et al.*, 2005). Interestingly, the G21R substitution is close to a consensus sequence present in Cx43 (residues 25–32) for putative binding to a Cav-1 scaffolding domain (ΦXΦXXXXΦ, where Φ is an aromatic amino acid [Phe, Tyr, or Trp]; (Lin *et al.*, 2003). The G60S substitution occurs in a highly conserved Cx43 amino acid within the first extra-
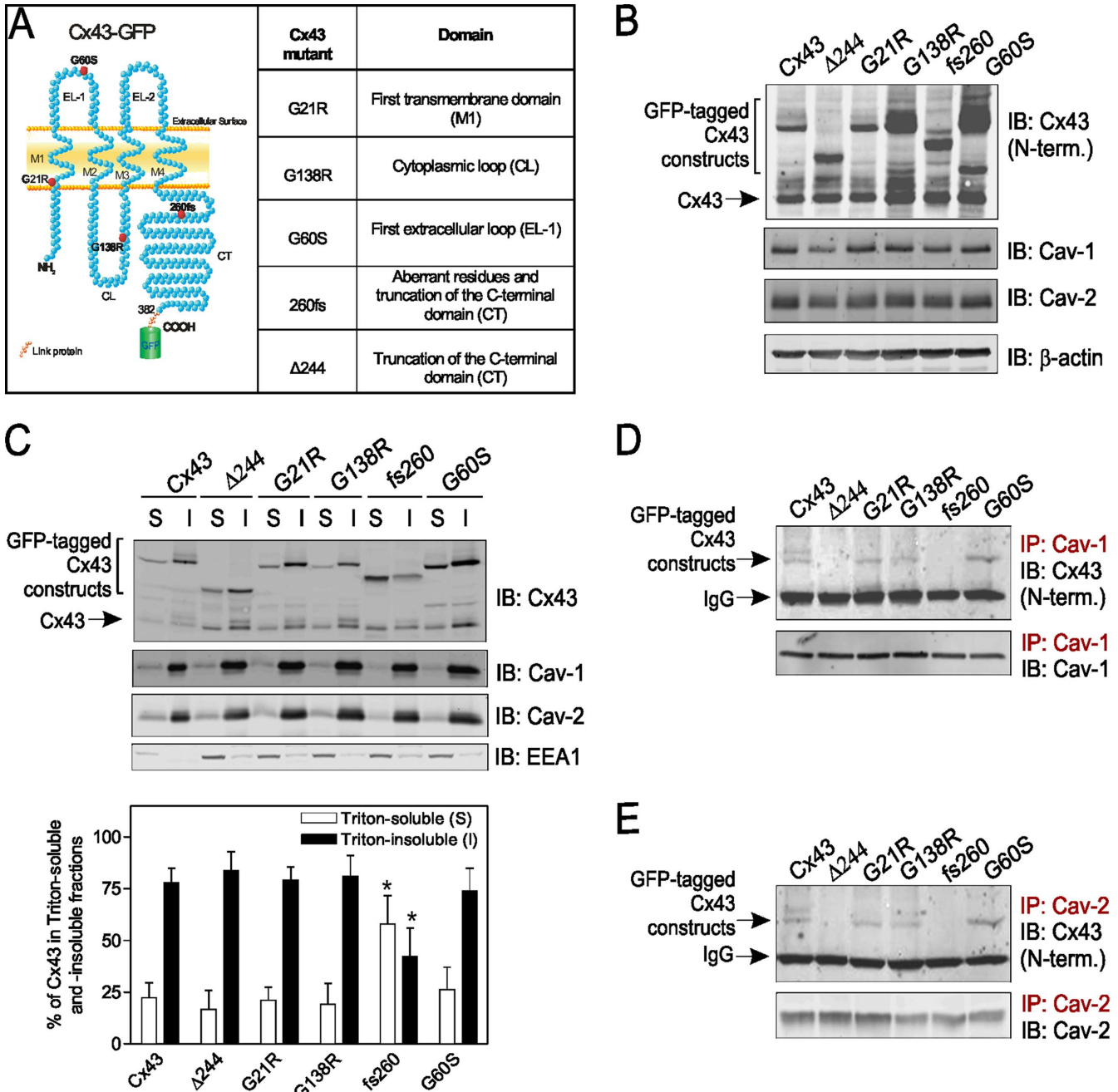
Figure 7. The C-terminal tail of Cx43 is required for its association with Cavs. (A) A predicted topology of GFP-tagged Cx43 depicting four transmembrane domains (M1–M4), two extracellular loops (EL-1 and EL-2), a cytoplasmic loop (CL), and an N terminus and a C terminus (CT) are shown. Similar to WT Cx43, the C-terminal domain of all the Cx43 mutants used in this study were fused to GFP. The G21R, G138R, and G60S are missense mutations present in the first transmembrane domain, the cytoplasmic loop, and the first extracellular loop, respectively. The fs260 mutant represents a frameshift where residues 260–305 are aberrant amino acid residues and in which the C-terminal domain is truncated. The Δ244 mutant is truncated after residue 243 in its C terminus. (B) REKs overexpressing Cx43-GFP or GFP-tagged Cx43 mutants were subjected to Western blot. β-Actin was used as a loading control. (C) Triton solubility of GFP-tagged Cx43 constructs in REKs overexpressing GFP-tagged WT Cx43 and mutants. Insoluble (I) and soluble (S) fractions were analyzed by Western blotting. EEA1 was used as a fractionation control. Amount of Cx43-GFP and GFP-tagged Cx43 mutants in each fraction was quantified, and data are expressed as percentage of Cx43 in Triton-soluble and -insoluble fractions (n = 3, *p < 0.05). Cx43-GFP and the G21R, G138R, and G60S mutants coimmunoprecipitated with Cav-1 (D) and Cav-2 (E), but not the Δ244 and fs260 mutants. An antibody directed against the N-terminal domain (NT1) of Cx43 was used to detect all the Cx43 constructs. If present in the Cavs immunoprecipitates, the Δ244 mutant would have been detected as a band just below the IgG heavy chain band, whereas the fs260 mutant would have been detected as a slightly higher band than the IgG band. IP, immunoprecipitation; IB, immunoblotting.

cellular loop, and it is the same mutation found in a mouse model of ODDD (Flenniken *et al.*, 2005). The fs260 mutant is the

result of a dinucleotide deletion (780–781del) in the *GJA1* gene resulting in a frame-shift, yielding 46 aberrant amino acids

after residue 259 and a shortened protein at residue 305 (van Steensel *et al.*, 2005). In a previous report, it was shown that two truncated Cx43 mutants at residues 257 and 374 could still interact with Cav-1 (Schubert *et al.*, 2002); thus, in our study, we included a substantially more truncated mutant (Δ244) to assess whether the C-terminal tail was required for binding to Cavs.

As shown in Figure 7B, all the Cx43 GFP-tagged constructs, including WT and mutants, were overexpressed in REKs without altering the expression levels of Cav-1 and -2. None of the mutants significantly affected endogenous Cx43 levels, except the fs260 mutant, which reduced Cx43 by ~30%. Similarly, all mutants except for fs260, behaved similar to WT Cx43, because they were predominantly Triton insoluble (Figure 7C), but none of them affected the Triton solubility of endogenous Cx43 (data not shown). These results are in accordance with our confocal imaging data in REKs demonstrating that the G21R, G138R, G60S, and Δ244 Cx43 mutants are found in intracellular compartment and at the plasma membrane within gap junction plaques, whereas the 260fs is retained in intracellular compartments (ER and Golgi apparatus) (Flenniken *et al.*, 2005; Roscoe *et al.*, 2005; Gong *et al.*, 2006). As opposed to WT Cx43 and the G21R, G138R, and G60S mutants, the Δ244 and fs260 mutants did not coimmunoprecipitate with Cav-1 (Figure 7D) or -2 (Figure 7E). Collectively, these data indicate that the intracellular C-terminal domain of Cx43 is required for its interaction with Cavs.

The C-terminal Tail of Cx43 Can Bind Directly to Cav-1

Cx43 has been shown to coimmunoprecipitate with exogenous Cav-1 in transfected 293T cells (Schubert *et al.*, 2002), which do not express any Cavs endogenously (Schlegel and Lisanti, 2000), suggesting that Cx43 can interact with Cav-1 independently of Cav-2. Because Cav-2 is known to form oligomers with Cav-1 (Scheiffele *et al.*, 1998), its interaction with Cx43 might be indirect and occurring through Cav-1. To investigate whether Cx43 can directly bind to Cav-1, Cav-1 immunoprecipitates from independent sets of Cav-1–transfected and untransfected 293T cells were incubated with a soluble carboxy-terminal fragment of Cx43 designated (Cx43CT) in a Far Western blotting approach. In Cav-1 immunoprecipitates only, Cx43CT bound to a band doublet at ~21–25 kDa (Figure 8, top, red). The same blot was then reprobed with anti-Cav-1 antibodies (middle, green), which strongly recognized a band at ~21 kDa and weakly recognized a second slightly higher molecular weight protein. These bands most likely correspond to the α and β isoforms of Cav-1. Taking advantage of the Odyssey infrared-imaging system, the overlay images revealed that the lower molecular weight band detected by Cx43CT corresponded to Cav-1 (bottom, yellow) suggesting that Cx43 directly binds to Cav-1.

Reduction of Cav-1 and -2 Expression by Using siRNA against Cav-1 Diminishes the Pool of Cx43 Present in Lipid Rafts and GJIC in REKs

To investigate the role of Cavs in regulating Cx43 expression, localization, or function, REKs were infected with a retrovirus expressing an RNAi targeting Cav-1. As shown in Figure 9A, Cav-1 expression was reduced by ~80% by using this approach. Cav-2 expression was also diminished by ~40%, which is accordance with previous reports showing that Cav-1 null or knockdown cells exhibit a loss in Cav-2 due to its degradation by the proteasome pathway (Razani *et al.*, 2001; Manninen *et al.*, 2005; Lin *et al.*, 2007). However, the expression and the overall phos-
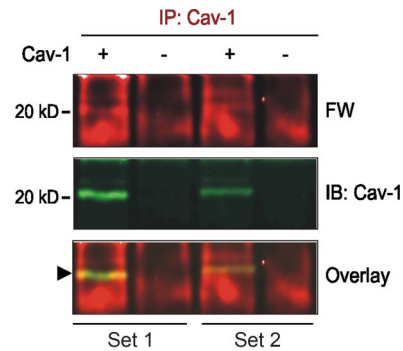

Figure 8. Cx43 can bind directly to Cav-1. Cav-1 was immunoprecipitated from two sets of Cav-1-transfected and untransfected 293T cells, and the immunoprecipitates were resolved by SDS-PAGE and transferred to nitrocellulose. The blot was probed with Cx43CT (Far Western [FW]), which bound to an ~21- to 25-kDa doublet only in immunoprecipitates from Cav-1–expressing cells (red, top). Bound Cx43CT was detected using antibodies against the C-terminal domain of Cx43. The blot was reprobed with anti-Cav-1 antibody (green, middle) and overlay images revealed that the Cx43CT bound to the same band detected with anti-Cav-1 antibodies (yellow, bottom).

phorylation profile of Cx43 were not affected by the reduction of Cavs levels (Figure 9A), as the ratio of the P_0 versus the P forms remained unchanged. Similar to Cav-1 and -2, the Triton solubility of Cx43 did not change in cells treated with Cav-1 siRNA (Figure 9B), compared with WT or control REKs, suggesting that reduction in Cavs expression does not modulate the overall translocation of Cx43 from the intercellular compartment to the plasma membrane or vice versa. To confirm this observation, endogenous Cx43 was labeled in Cavs-knockdown REKs. Although the detection of endogenous Cx43 at the plasma membrane (Figure 9C, green, arrowheads) was not as strong as overexpressed Cx43-GFP, no obvious visual change in the overall Cx43 localization within these cells could be observed compared with control REKs. Indeed, endogenous Cx43 was present at the plasma membrane (Figure 9C, arrowheads) and in intracellular compartments (Figure 9C, arrows) in both control and Cavs-knockdown REKs. The localization of endogenous Cx43 was also similar in these cells when Cx43 was labeled using the P4G9 antibody, which has high affinity for Cx43 at the plasma membrane (Figure 9D). Although reduction in Cavs expression did not lead to obvious change in Cx43 localization at the cell surface, we assessed whether it might have a more subtle effect that could not be observed by confocal microscopy such as the targeting of Cx43 within lipid rafts. These domains were thus isolated from control (Figure 9E) and Cavs-reduced REKs (Figure 9F), and the presence of Cx43, Cav-1, and Cav-2 was determined by Western blotting. The presence of Cx43 and Cavs in raft (R) and in nonraft fractions (NR) was also assessed in pooled fractions 4–6 (R) and in pooled fractions 8–12 (NR) loaded at equal amount of proteins (Figure 9G). Although the amounts of Cavs were lower in Cavs-reduced REKs, the proportion or percentage of Cav-1 and -2 present in rafts remained similar (Figure 9G). Interestingly, the percentage of Cx43 present in the raft fraction was diminished in Cavs-reduced REKs (29.7 ± 3.4%), compared with control cells (41.3 ± 5.6%, $p < 0.05$, $n = 4$) (Figure 9H). Taking into account the confocal imaging and Triton solubility data from control and Cavs-reduced REKs, our results suggest that the over-
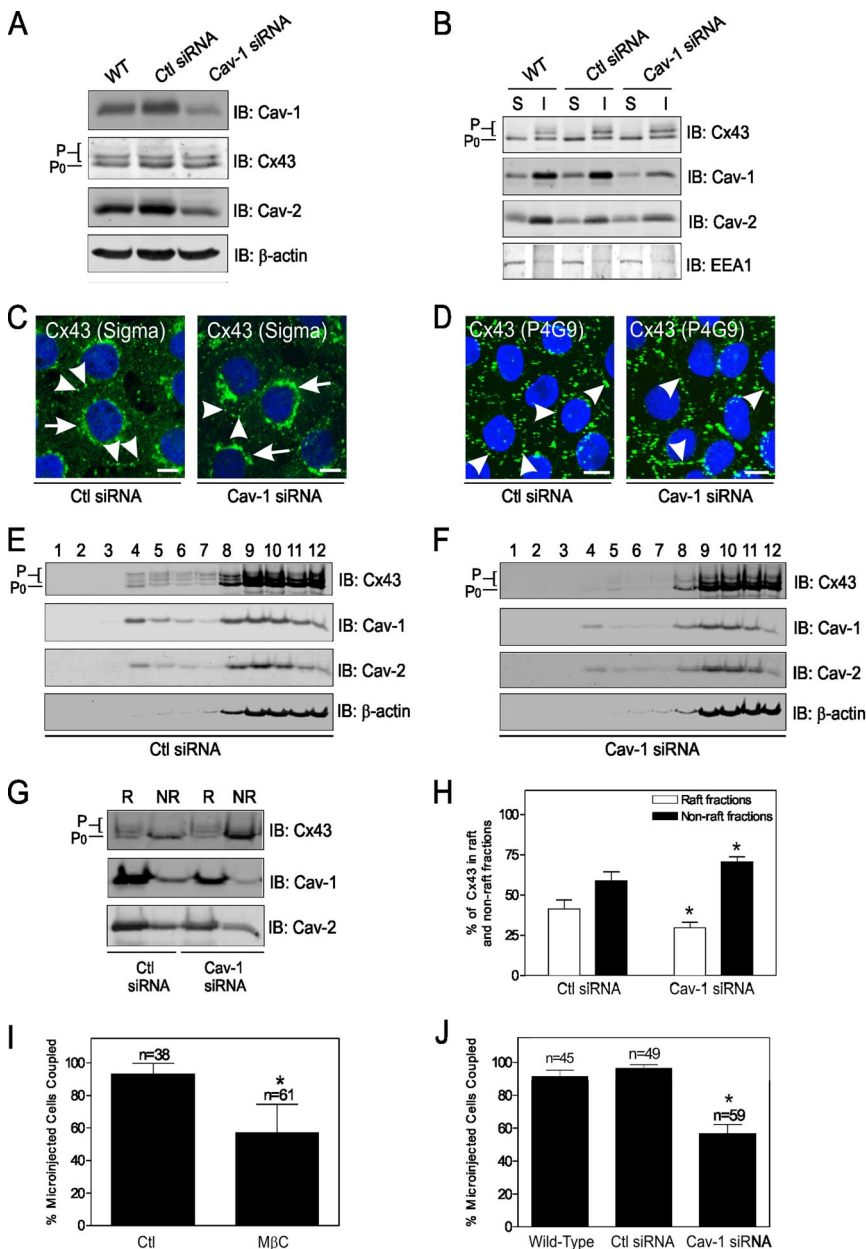
Figure 9. RNAi knockdown of Cav-1 and -2 expression reduces the pool of Cx43 present in lipid rafts and GJIC in REKs. WT REKs were infected with a retrovirus encoding a control (Ctl) RNAi, or an RNAi targeting Cav-1. (A) Western blot show that Cav-1 and Cav-2 expression was reduced by ~80 and ~40%, respectively, whereas Cx43 level remained unchanged in cells treated with Cav-1 siRNA. β-actin was used as a loading control. (B) Triton solubility of Cx43, Cav-1, and Cav-2. EEA1 was used as a fractionation control. S, soluble fractions; I, insoluble fractions. (C) Labeling of endogenous Cx43 by using an anti-Cx43 antibody obtained from Sigma (green) revealed its location within intracellular compartments (arrows) and at the plasma membrane (arrowheads) in both Ctl and Cavs-knockdown REKs. (D) Labeling of endogenous Cx43 by using the P4G9 anti-Cx43 antibody (green) mainly detected Cx43 at the plasma membrane (arrowheads) in both Ctl and Cavs-knockdown REKs. (E) Ctl and (F) Cavs-knockdown REKs were subjected to sucrose density gradient centrifugation. Twelve fractions were collected and analyzed by Western blot. (G) Fractions 4–6 (R) and fractions 8–12 (NR) were pooled, and equal amounts of proteins were submitted to Western blotting. (H) Percentage of Cx43 present in raft (fractions 4–6) and in nonraft fractions (8–12) were quantified when equal amounts of proteins were analyzed by Western blotting (n = 4, *p < 0.05 compared with the equivalent fractions in control cells). (I) Untreated and MβC-treated WT REKs were microinjected with Lucifer yellow. Data were expressed as percentage of microinjected cells that passed dye (n represents the number of microinjected cells from three independent experiments, *p < 0.05). (J) WT, Ctl REKs, or REKs that were infected with Cav-1 siRNA were microinjected with Lucifer yellow. Data are expressed as percentage of microinjected cells that passed dye (n represents the number of microinjected cells from three independent experiments, *p < 0.001 compared with WT and Ctl REKs).

all presence of Cx43 at the plasma membrane was not altered when Cavs level were reduced, but a smaller proportion of Cx43 was found in lipid rafts.

We then evaluated whether raft domains and Cavs play a role in regulating GJIC. Treatment of REKs with MβC, which induced the translocation of Cx43 and Cavs into Triton-soluble fractions (Figure 6B), and reduced the Cx43/Cavs association (Figure 6, I and J), significantly inhibited GJIC (Figure 9I). To assess the role of caveolins in this process, dye-coupling studies were performed in Cavs-knockdown REKs. Reduction in Cav-1 and -2 expression by using Cav-1 siRNA resulted in a significant inhibition of GJIC compared with WT and control cells (Figure 9J). Together, these data indicate that Cavs plays a role in regulating GJIC through a mechanism that does not seem to involve direct regulation of the expression of Cx43, its overall phosphorylation, or presence at the plasma membrane, but rather its targeting into lipid rafts.

Overexpression of Cav-1 Induces the Translocation of Cx43 into Lipid Rafts and GJIC in 293T Cells

To further examine the relationship between Cavs and Cx43, we overexpressed Cav-1 in 293T cells, which express Cx43 (Figure 10A) but have no detectable levels of any known caveolin (Schlegel and Lisanti, 2000). Consistent with our results in REKs, overexpression of Cav-1 in 293T cells did not alter Cx43 expression and/or overall phosphorylation level (Figure 10A). Cav-2 was not detected by Western blotting in either WT or Cav-1–overexpressing 293T cells (data not shown). As reported previously (Schubert *et al.*, 2002), Cx43 and Cav-1 were predominantly Triton-insoluble in these cells (Figure 10B). Confirming our results obtained from Cavs-knockdown REKs, the overexpression of Cav-1 did not alter the Triton solubility of Cx43 (Figure 10B). Accordingly, Cx43 reached the plasma membrane and could form gap junc-
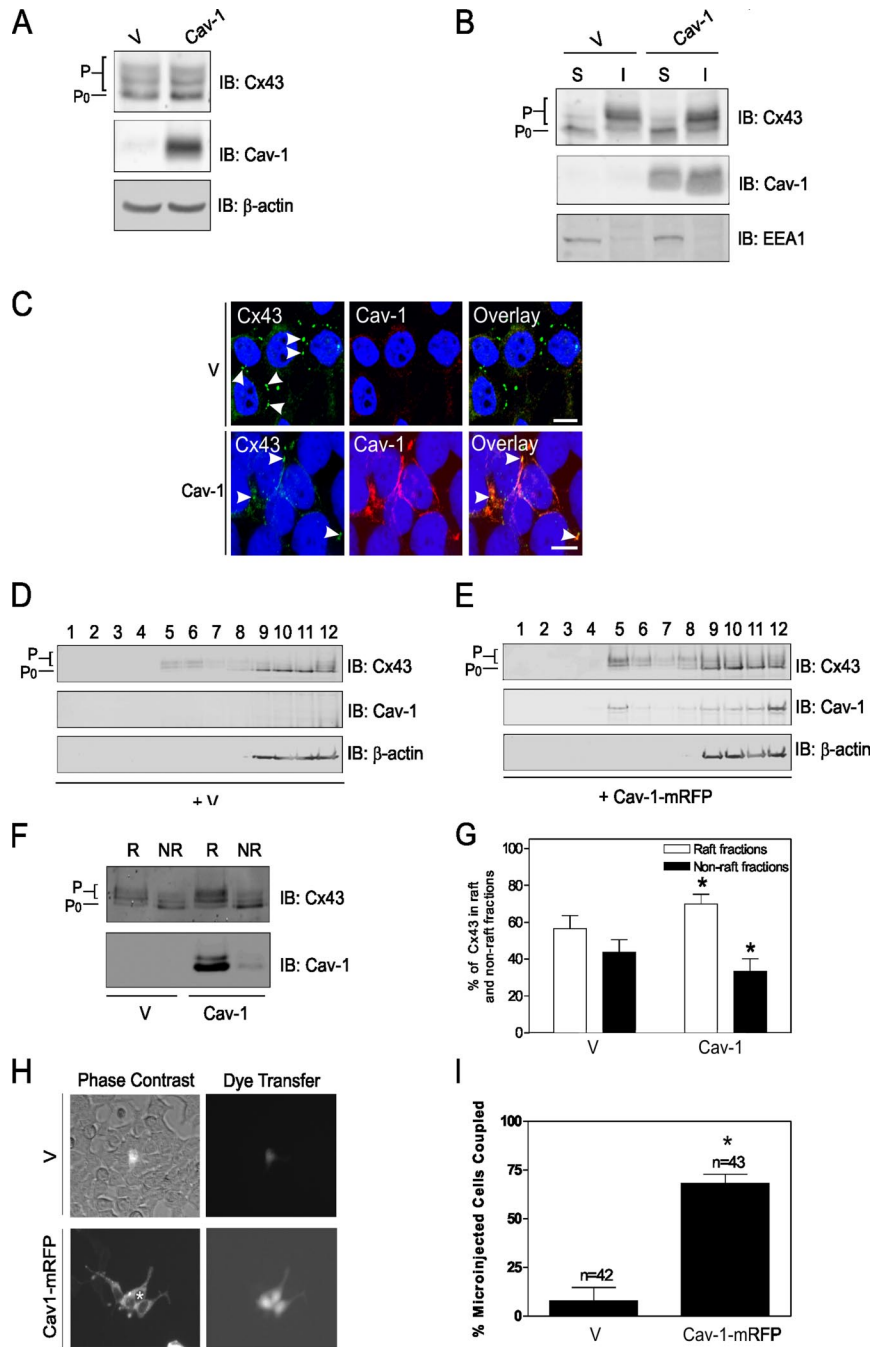
Figure 10. Overexpression of Cav-1 in 293T cells induces the translocation of Cx43 into lipid rafts and increases GJIC. 293T cells were transfected with Cav-1 or the empty vector (V), subjected to Western blotting, and probed for Cx43 and Cav-1 (A). β-Actin was used as a loading control. (B) Triton solubility of Cx43 and Cav-1. EEA1 was used as a fractionation control. S, soluble fraction; I, insoluble fractions. (C) 293T cells were transfected with Cav-1 or control empty vector (V) and labeled for Cx43 (P4G9 anti-Cx43 antibody, green) and Cav-1 (red). Confocal imaging of control 293T cells (top) revealed Cx43 at the cell surface (arrowheads) in the absence of Cav-1. No obvious difference was observed in Cx43 localization at the plasma membrane (arrowheads) in Cav-1–expressing 293T cells, compared with control cells (V). Overlay images suggest that a population of Cx43 at the plasma membrane colocalizes with Cav-1 (yellow, bottom, arrowheads). (D) Control empty vector (V) and (E) Cav-1–transfected 293T cells were subjected to sucrose density gradient centrifugation. Twelve fractions were collected and analyzed by Western blot. (F) Fractions 4–6 (R) and fractions 8–12 (NR) were pooled, and equal amounts of proteins were submitted to Western blotting. (G) Percentage of Cx43 present in raft (fractions 4–6) and in nonraft fractions (8–12) were quantified when equal amounts of proteins were analyzed by Western blotting (n = 3, *p < 0.05 compared with the equivalent fractions in cells transfected with the empty vector). (H) 293T cells were transfected with Cav-1-mRFP or control empty vector (V) and microinjected with Lucifer yellow. (I) Data are expressed as percentage of microinjected transfected cells that passed dye (n represents the number of microinjected cells from three independent experiments, *p < 0.05). Blue, nuclei. Bars, 10 μm.

tion plaques in control 293T cells (Figure 10C, green, top, arrowheads), suggesting that these processes do not strictly depend on Cav-1. In addition, no obvious difference in Cx43 localization was observed between control and Cav-1–overexpressing 293T cells by using the P4G9 antibody, which mainly recognizes Cx43 at the plasma membrane (Figure 10C). Although the majority of exogenous Cav-1 was not colocalized with Cx43, overlay images suggest that a small population of Cx43 colocalizes with Cav-1 at the cell surface (Figure 10C, bottom, arrowheads). To confirm that Cav-1 plays a role in targeting Cx43 into lipid raft domains, raft and nonraft membrane fractions were isolated from control (Figure 10D) and Cav-1–transfected 293T cells (Figure 10E), and the pres-

ence of Cx43 and Cav-1 were evaluated by Western blotting. The presence of Cx43 in R and in NR fractions was also assessed in pooled fractions (4–6 [R] and 8–12 [NR]) loaded at equal amount of proteins (Figure 10F). Cx43 was detected in lipid raft fractions in control 293T cells (Figure 10F), but the proportion present in these microdomains was slightly increased in cells overexpressing Cav-1 (Figure 10G, 67.0 ± 6.6% compared with 56.5 ± 7.0% in control cells; p < 0.05, n = 3). To further confirm the results obtained using REKs, we then tested whether Cav-1 overexpression could stimulate GJIC. We found that although 293T cells express low levels of endogenous Cx43, these cells were poorly coupled, because only ~10% of microinjected cells passed Lucifer yellow dye (Figure

10, H and I). Interestingly, ~70% of microinjected cells overexpressing Cav-1-mRFP passed dye (Figure 10, H and I), confirming that Cav-1 regulates GJIC.

DISCUSSION

Our results indicate that Cx43 coimmunoprecipitates and colocalizes with Cav-1 and -2 in REKs. Interestingly, the various phosphorylated species of Cx43, and the P_0 species, were found to associate with Cavs. It is thought that the Triton-soluble P_0 form of Cx43 assembles into connexons en route to the plasma membrane and that most phosphorylation events occur subsequent to delivery of connexons into Triton-insoluble gap junction plaques (Musil and Goodenough, 1991; Musil and Goodenough, 1993; Solan and Lampe, 2005). Similar to Cx43, Cavs are synthesized in the ER, transported to the Golgi and then to the cell surface in Triton-insoluble domains (Parton *et al.*, 2006). Because the Triton-soluble P_0 form of Cx43 corresponds to a pool found in intracellular compartments, its interaction with Cavs most likely occurs when Cx43 has reached the Golgi apparatus. In addition to our colocalization data, the Cx43/Cavs association in the Golgi complex was confirmed by coimmunoprecipitation experiments in BFA-treated cells. Although the majority of the colocalization of Cx43 with Cavs was observed in the Golgi, our biotinylation and coimmunoprecipitation experiments indicate that a second population of Cx43 interacts with Cavs at the cell surface. Treatment with MβC reduced the Cx43/Cavs association further indicating that, in addition to the Golgi apparatus, a portion of the Cx43/Cavs complex is present at the plasma membrane in lipid rafts/caveolae.

The Golgi complex has been identified as the site where newly assembled caveolae domains occur first before their rapid vesicular delivery to the plasma membrane where they insert as a stable caveolar domain (Tagawa *et al.*, 2005). It is thought that Cav-1 and -2 hetero-oligomers represent the assembly units that drive caveolae formation. In the *trans*-Golgi network of epithelial cells, Cav-1/-2 hetero-oligomers have been reported to be sorted into basolateral vesicles and formed caveolae, whereas caveolae were not normally observed on the apical surface when only Cav-1 was found (Scheiffele *et al.*, 1998). The formation of a Cav-1/-2 hetero-oligomeric complex has been shown to be required for Cav-2 transport from the Golgi to the plasma membrane in caveolae (Parolini *et al.*, 1999). Our confocal data indicate that the majority of Cav-1 and -2 are colocalized in the Golgi apparatus and at the plasma membrane, suggesting that they mainly exist as hetero-oligomers in REKs. In addition, Cx43 and Cav-1 were both found in Cav-2 immunoprecipitates, suggesting that Cx43 interacts with these Cav-1/-2 hetero-oligomers. Our biotinylation experiments further indicate that a portion of the complex formed of Cx43 and Cav-1/-2 hetero-oligomers is present at the cell surface. These Cav complexes seemed to be stable because BFA and MβC treatment did not alter the association between Cav-1 and -2, but it led to a significant dissociation of Cx43 from Cavs. Taking into account previous studies on caveolae biogenesis (Scheiffele *et al.*, 1998; Parolini *et al.*, 1999; Tagawa *et al.*, 2005; Parton *et al.*, 2006), our results suggest that Cx43 is associated with Cavs in newly assembled caveolae, which exit the Golgi and most likely traffic together to be delivered in lipid rafts/caveolae at the plasma membrane. Cavs would thus be involved in the exocytic transport of Cx43, rather than in its internalization from the plasma membrane.

Caveolae assembled in the Golgi do not exchange caveolin molecules with each other or with any other pool once they reach the cell surface. In resting cells, caveolae at the cell surface are mainly immobile because they are tightly associated with the actin cytoskeleton and microfilaments (Tagawa *et al.*, 2005). Our confocal data indicate that the majority of Cx43 and Cavs are not colocalized at the cell surface, suggesting that the Cx43/Cavs complex dissociate after its delivery in lipid rafts to the plasma membrane. Accordingly, it has been suggested that nonjunctional Cx26 and Cx32 are present in lipid rafts and that rafts might be involved in trafficking of plasma membrane connexin channels to gap junctions (Locke *et al.*, 2005). Similarly, a model has been proposed in which connexons are delivered to the plasma membrane and reside transiently in lipid raft domains, requiring the tight junction protein zona occludens (ZO)-1 for recruitment into gap junctional plaques. Because ZO-1 is an actin binding protein, interactions with the actin cytoskeleton may also be involved in the recruitment of connexins to gap junctions (Laing *et al.*, 2005). In keeping with our work, little Cx43 would thus reside in lipid rafts under steady-state conditions.

Our mutational analysis of Cx43 indicates that its C-terminal tail is involved in its interaction with Cavs. Indeed, the Δ244 mutant, which is almost completely truncated of its intracellular C-terminal domain, did not coimmunoprecipitate with Cavs. Similar to WT Cx43, this mutant was found in a Golgi-like intracellular compartment and within gap junction plaques (data not shown). These findings, combined with our confocal data of Cx43 localization in control 293T cells, indicate that Cavs are not essential for Cx43 transport to the cell surface. The trafficking of the GFP-tagged Δ244 mutant is also independent of the presence of wild-type Cx43, because it can reach the plasma membrane when expressed in Cx-negative HeLa cells (data not shown). Because the Δ244 mutant behaved similarly to WT Cx43 regarding its cellular localization and Triton solubility, its lack of interaction with Cavs was not due to a defect in its trafficking or lack of targeting to detergent-insoluble domains. Confirming the results obtained using the Δ244 mutant, the fs260 mutant did not coimmunoprecipitate with Cavs. Our data obtained using the Δ244 and fs260 mutants differed somewhat from those of Schubert *et al.* (2002) in which another Cx43 mutant partially truncated in its C-terminal tail could still be immunoprecipitated with Cav-1. Interestingly, the majority of the fs260 mutant is localized in the endoplasmic reticulum and only minimal localization was found in the Golgi or at the cell surface (Gong *et al.*, 2006) where the interaction of Cx43 with Cavs normally occurs. In addition, the 46 aberrant amino acids and the shortening of the C-terminal domain of the fs260 mutant (van Steensel *et al.*, 2005) might modify its conformation in a way that would not allow an interaction with Cavs. The difference in the ability of the M257 mutant to interact with Cav-1, as opposed to the Δ244 mutant, might also suggest that the portion of the Cx43 C-tail that is important for its interaction with Cavs is between residues 244–256. The role of the C-terminal domain of Cx43 (CT) in the Cx43/Cav-1 interaction has been confirmed using a Far Western analysis, which demonstrated that Cx43CT can bind directly and specifically to Cav-1 and that the lack of interaction of the Δ244 mutant with Cavs is not due to the presence of the GFP tag. Importantly, the C-terminal domain of Cx43 is thought to be crucial in the control of gap junction function via phosphorylation-dependent control of gap junction assembly and gating (Shin *et al.*, 2001), and through its interaction

with other binding partners, including ZO-1 (Toyofuku *et al.*, 1998), ZO-2 (Singh *et al.*, 2005), and NOV (Gellhaus *et al.*, 2004). However, our mutational analysis does not rule out a possible involvement of other domains of Cx43, as point mutations (G21R, G138R, and G60S) might not be sufficient to disrupt the Cx43/Cavs interaction.

To understand the role of Cavs and their interaction with Cx43, we generated REKs that were reduced by ~80% in Cav-1 and ~40% in Cav-2 contents by using siRNA against Cav-1, and we overexpressed Cav-1 in Cavs-deficient 293T cells. Our data indicate that modulation of Cavs level in these cells did not affect Cx43 expression or overall phosphorylation. In addition, reduction in Cavs expression in REKS and overexpression of Cav-1 in 293T cells did not induce the translocation of Cx43 between Triton-soluble and -insoluble fractions or affect the overall ability of Cx43 to be transported to the plasma membrane. Furthermore, no obvious visible change in Cx43 localization could be observed in these cells compared with their control counterparts. However, although the reduction of Cavs in caveolin-knockdown REKs did not affect Cx43 expression or its ability to reach the plasma membrane, it was sufficient to significantly diminish the proportion of Cx43 targeted to lipid rafts, and GJIC. We propose that the reduction in Cavs level, and the accompanying Cx43/Cavs interactions, dysregulates the targeting of Cx43 into lipid rafts, which leads to an overall reduction in GJIC. In further support of this concept, the presence of Cx43 in lipid rafts at the plasma membrane likely plays a role in regulating its communication function, as suggested by the inhibition of GJIC by MβC treatment. The importance of Cav-1 in translocating Cx43 into lipid rafts microdomains and regulating GJIC was confirmed using 293T cells. In the absence of Cav-1, Cx43 still reached the plasma membrane, and a proportion was targeted into lipid rafts, which was increased upon Cav-1 expression. Interestingly, our results demonstrated that 293T cells are poorly coupled but that overexpression of Cav-1 strongly increases their communication status. This effect was most likely due to Cav-1, because no detectable level of Cav-2 could be observed in WT or Cav-1 overexpressing 293T cells. Accordingly, reduction of Cav-2 level by ~45% by using siRNA did not modulate GJIC in REKs (data not shown), suggesting that the diminution of GJIC observed in Cavs-reduced REKs was most likely due to a reduction in Cav-1 levels rather than Cav-2. However, these data cannot exclude a role of Cav-2 in regulating GJIC, because the reduction of its expression might have been insufficient. Thus, these data support the existence of a GJIC regulatory event that occurs after Cavs-mediated delivery of Cx43 to the cell surface into lipid rafts, and most likely before the assembly of a detergent-resistant gap junction plaque. In addition to the targeting of Cx43 to lipid rafts, the effect of Cav-1 on the regulation of GJIC might involve additional mechanisms, because caveolins can also act independently of caveolae (Head and Insel, 2007).

Other types of channels have been reported to be functionally regulated by Cav-1 (Trouet *et al.*, 1999; Trouet *et al.*, 2001; Toselli *et al.*, 2005; Wang *et al.*, 2005; Kwiatek *et al.*, 2006; Remillard and Yuan, 2006). As shown previously in its interaction with Cx43 (Schubert *et al.*, 2002), the scaffolding domain (CSD) of Cav-1 has been involved in its binding to the TRCP1 channel (Wang *et al.*, 2005; Remillard and Yuan, 2006). According to the caveolae signaling hypothesis, Cav-1 interacts with and regulates the activity of caveolae-associated proteins via its CSD (Schlegel *et al.*, 2000). The presence of Cx43 in lipid rafts, which are enriched in signaling mol-

ecules, and its interaction with Cav-1 CSD provide potential avenues by which Cav-1 may participate in a signal transduction cascade involved in regulating the communication function of Cx43. The interaction of Cav-1 with Cx43 has also been shown to require the C-terminal domain of Cav-1 (Schubert *et al.*, 2002). Because the CT domain of Cx43 does not contain a known consensus sequence for binding to a Cav-1 scaffolding domain, it might interact with the C-terminal domain of Cav-1. This domain possesses a membrane attachment domain, which directs Cav-1 localization to the *trans*-Golgi network (Hnasko and Lisanti, 2003). The requirement of the C-terminal domain of Cav-1 in its association with Cx43 further strengthens the importance of the Golgi localization for this interaction to occur.

The association between Cx43 and caveolins found in REKs was also observed in vivo as Cx43 and Cav-1 colocalized in keratinocytes from human skin epidermis, suggesting that this association is physiologically relevant. Although the colocalization of Cav-1 and -2 has been reported in various cell types and tissues, the interaction between Cx43 and Cav-2 could not be assessed in human epidermis due to a lack of specific Cav-2 staining by using different commercially available antibodies. During the differentiation of the epidermis, proliferation of keratinocytes is restricted to the basal layer (Candi *et al.*, 2005). The colocalization of Cx43 with Cav-1 was mainly observed in the spinosum layer of the epidermis, suggesting that the Cx43/Cavs interaction is regulated during epidermal differentiation. Interestingly, the only two Cx43 mutants used in the present study that did not coimmunoprecipitate with Cavs were the fs260 ODDD-linked mutant and a C-terminal tail truncation of Cx43 (Δ244). Although ODDD patients are usually not affected with skin symptoms, the fs260 mutation has been reported to be associated with palmoplantar keratoderma (van Steensel *et al.*, 2005). More recently, it has been shown that skin changes in ODDD are correlated with C-terminal truncations of Cx43 (Vreeburg *et al.*, 2007). Together, these data suggest that the association of Cx43 with Cav-1 in keratinocytes might play a functional role during epidermal differentiation.

In summary, we demonstrate that Cx43 interacts with Cav-1 and Cav-2 in REKs, thus identifying Cav-2 as a new Cx43 interacting partner possibly via its binding to Cav-1. Mutation and Far Western analyses identified that the CT of Cx43 is a required domain for the Cx43/Cavs interaction to occur and that Cx43CT can bind directly to Cav-1. Our results indicate that newly synthesized Cx43 interacts with Cavs in the Golgi complex, and suggest that they traffic together to the plasma membrane in lipid rafts. Although a population of Cx43 is found associated with Cavs in lipid rafts at the plasma membrane, our data suggest that the majority of Cx43 dissociates from Cavs once at the cell surface before gap junction plaque formation. Finally, our results showed that caveolins, most likely through their association with Cx43 and its subsequent targeting in lipid rafts, play a role in regulating GJIC.

REFERENCES

Balijepalli, R. C., Foell, J. D., Hall, D. D., Hell, J. W., and Kamp, T. J. (2006). Localization of cardiac L-type Ca(2+) channels to a caveolar macromolecular signaling complex is required for beta(2)-adrenergic regulation. Proc. Natl. Acad. Sci. USA *103*, 7500–7505.

Barbuti, A., Gravante, B., Riolfo, M., Milanesi, R., Terragni, B., and DiFrancesco, D. (2004). Localization of pacemaker channels in lipid rafts regulates channel kinetics. Circ. Res. *94*, 1325–1331.

Barth, K., Gentsch, M., Blasche, R., Pfuller, A., Parshyna, I., Koslowski, R., Barth, G., and Kasper, M. (2005). Distribution of caveolin-1 and connexin43 in normal and injured alveolar epithelial R3/1 cells. Histochem. Cell Biol. *123*, 239–247.

Brainard, A. M., Miller, A. J., Martens, J. R., and England, S. K. (2005). Maxi-K channels localize to caveolae in human myometrium: a role for an actin-channel-caveolin complex in the regulation of myometrial smooth muscle K+ current. Am. J. Physiol. *289*, C49–C57.

Brazer, S. C., Singh, B. B., Liu, X., Swaim, W., and Ambudkar, I. S. (2003). Caveolin-1 contributes to assembly of store-operated Ca2+ influx channels by regulating plasma membrane localization of TRPC1. J. Biol. Chem. *278*, 27208–27215.

Breuza, L., Corby, S., Arsanto, J. P., Delgrossi, M. H., Scheiffele, P., and Le Bivic, A. (2002). The scaffolding domain of caveolin 2 is responsible for its Golgi localization in Caco-2 cells. J. Cell Sci. *115*, 4457–4467.

Bush, W. S., Ihrke, G., Robinson, J. M., and Kenworthy, A. K. (2006). Antibody-specific detection of caveolin-1 in subapical compartments of MDCK cells. Histochem. Cell Biol. *126*, 1–8.

Candi, E., Schmidt, R., and Melino, G. (2005). The cornified envelope: a model of cell death in the skin. Nat. Rev. Mol. Cell Biol. *6*, 328–340.

Capozza, F., Williams, T. M., Schubert, W., McClain, S., Bouzahzah, B., Sotgia, F., and Lisanti, M. P. (2003). Absence of caveolin-1 sensitizes mouse skin to carcinogen-induced epidermal hyperplasia and tumor formation. Am. J. Pathol. *162*, 2029–2039.

Cascio, M. (2005). Connexins and their environment: effects of lipids composition on ion channels. Biochim. Biophys. Acta *1711*, 142–153.

Cohen, A. W., Hnasko, R., Schubert, W., and Lisanti, M. P. (2004). Role of caveolae and caveolins in health and disease. Physiol. Rev. *84*, 1341–1379.

Cohen, A. W., Razani, B., Wang, X. B., Combs, T. P., Williams, T. M., Scherer, P. E., and Lisanti, M. P. (2003). Caveolin-1-deficient mice show insulin resistance and defective insulin receptor protein expression in adipose tissue. Am. J. Physiol. *285*, C222–C235.

Estall, J. L., Yusta, B., and Drucker, D. J. (2004). Lipid raft-dependent glucagon-like peptide-2 receptor trafficking occurs independently of agonist-induced desensitization. Mol. Biol. Cell *15*, 3673–3687.

Fitzgerald, D. J., Fusenig, N. E., Boukamp, P., Piccoli, C., Mesnil, M., and Yamasaki, H. (1994). Expression and function of connexin in normal and transformed human keratinocytes in culture. Carcinogenesis *15*, 1859–1865.

Flenniken, A. M. *et al.* (2005). A Gja1 missense mutation in a mouse model of oculodentodigital dysplasia. Development *132*, 4375–4386.

Fujimoto, T., Kogo, H., Ishiguro, K., Tauchi, K., and Nomura, R. (2001). Caveolin-2 is targeted to lipid droplets, a new "membrane domain" in the cell. J. Cell Biol. *152*, 1079–1085.

Galbiati, F. *et al.* (1998). Expression of caveolin-1 and -2 in differentiating PC12 cells and dorsal root ganglion neurons: caveolin-2 is up-regulated in response to cell injury. Proc. Natl. Acad. Sci. USA *95*, 10257–10262.

Galipeau, J. L., H., Paquin, A., Sicilia, F., Karpati, G., Nalbantoglu, J. (1999). Vesicular Stomatis Virus G pseudotyped retrovector mediates effective in vivo suicide gene delivery in experimental brain cancer. Cancer Res. *59*, 2384–2394.

Gellhaus, A. *et al.* (2004). Connexin43 interacts with NOV: a possible mechanism for negative regulation of cell growth in choriocarcinoma cells. J. Biol. Chem. *279*, 36931–36942.

Giocondi, M. C., Milhiet, P. E., Dosset, P., and Le Grimellec, C. (2004). Use of cyclodextrin for AFM monitoring of model raft formation. Biophys. J. *86*, 861–869.

Goldberg, G. S., Moreno, A. P., and Lampe, P. D. (2002). Gap junctions between cells expressing connexin 43 or 32 show inverse permselectivity to adenosine and ATP. J. Biol. Chem. *277*, 36725–36730.

Gong, X. Q., Shao, Q., Lounsbury, C. S., Bai, D., and Laird, D. W. (2006). Functional characterization of a GJA1 frameshift mutation causing oculodentodigital dysplasia and palmoplantar keratoderma. J. Biol. Chem. *281*, 31801–31811.

Head, B. P., and Insel, P. A. (2007). Do caveolins regulate cells by action outside of caveolae? Trends Cell Biol. *17*, 51–57.

Hnasko, R., and Lisanti, M. P. (2003). The biology of caveolae: lessons from caveolin knockout mice and implications for human disease. Mol. Interv. *3*, 445–464.

Kamibayashi, Y., Oyamada, Y., Mori, M., and Oyamada, M. (1995). Aberrant expression of gap junction proteins (connexins) is associated with tumor progression during multistage mouse skin carcinogenesis in vivo. Carcinogenesis *16*, 1287–1297.

Kretz, M., Maass, K., and Willecke, K. (2004). Expression and function of connexins in the epidermis, analyzed with transgenic mouse mutants. Eur. J. Cell Biol. *83*, 647–654.

Kwiatek, A. M., Minshall, R. D., Cool, D. R., Skidgel, R. A., Malik, A. B., and Tiruppathi, C. (2006). Caveolin-1 regulates store-operated Ca2+ influx by binding of its scaffolding domain to transient receptor potential channel-1 in endothelial cells. Mol. Pharmacol. *70*, 1174–1183.

Laing, J. G., Chou, B. C., and Steinberg, T. H. (2005). ZO-1 alters the plasma membrane localization and function of Cx43 in osteoblastic cells. J. Cell Sci. *118*, 2167–2176.

Laird, D. W. (2005). Connexin phosphorylation as a regulatory event linked to gap junction internalization and degradation. Biochim. Biophys. Acta *1711*, 172–182.

Laird, D. W. (2006). Life cycle of connexins in health and disease. Biochem. J. *394*, 527–543.

Laird, D. W., Castillo, M., and Kasprzak, L. (1995). Gap junction turnover, intracellular trafficking, and phosphorylation of connexin43 in brefeldin A-treated rat mammary tumor cells. J. Cell Biol. *131*, 1193–1203.

Langlois, S., Maher, A. C., Manias, J. L., Shao, Q., Kidder, G. M., and Laird, D. W. (2007). Connexin levels regulate keratinocyte differentiation in the epidermis. J. Biol. Chem. *282*, 30171–30180.

Lauf, U., Giepmans, B. N., Lopez, P., Braconnot, S., Chen, S. C., and Falk, M. M. (2002). Dynamic trafficking and delivery of connexons to the plasma membrane and accretion to gap junctions in living cells. Proc. Natl. Acad. Sci. USA *99*, 10446–10451.

Lin, D., Lobell, S., Jewell, A., and Takemoto, D. J. (2004). Differential phosphorylation of connexin46 and connexin50 by H2O2 activation of protein kinase Cgamma. Mol. Vis. *10*, 688–695.

Lin, D., Zhou, J., Zelenka, P. S., and Takemoto, D. J. (2003). Protein kinase Cgamma regulation of gap junction activity through caveolin-1-containing lipid rafts. Invest. Ophthalmol. Vis. Sci. *44*, 5259–5268.

Lin, M. I., Yu, J., Murata, T., and Sessa, W. C. (2007). Caveolin-1-deficient mice have increased tumor microvascular permeability, angiogenesis, and growth. Cancer Res. *67*, 2849–2856.

Lisanti, M. P., Scherer, P. E., Vidugiriene, J., Tang, Z., Hermanowski-Vosatka, A., Tu, Y. H., Cook, R. F., and Sargiacomo, M. (1994). Characterization of caveolin-rich membrane domains isolated from an endothelial-rich source: implications for human disease. J. Cell Biol. *126*, 111–126.

Locke, D., Liu, J., and Harris, A. L. (2005). Lipid rafts prepared by different methods contain different connexin channels, but gap junctions are not lipid rafts. Biochemistry *44*, 13027–13042.

Lockwich, T. P., Liu, X., Singh, B. B., Jadlowiec, J., Weiland, S., and Ambudkar, I. S. (2000). Assembly of Trp1 in a signaling complex associated with caveolin-scaffolding lipid raft domains. J. Biol. Chem. *275*, 11934–11942.

Maass, K. *et al.* (2004). Defective epidermal barrier in neonatal mice lacking the C-terminal region of connexin43. Mol. Biol. Cell *15*, 4597–4608.

Maher, A. C., Thomas, T., Riley, J. L., Veitch, G., Shao, Q., and Laird, D. W. (2005). Rat epidermal keratinocytes as an organotypic model for examining the role of Cx43 and Cx26 in skin differentiation. Cell Commun. Adhes. *12*, 219–230.

Mao, A. J., Bechberger, J., Lidington, D., Galipeau, J., Laird, D. W., and Naus, C. C. (2000). Neuronal differentiation and growth control of neuro-2a cells after retroviral gene delivery of connexin43. J. Biol. Chem. *275*, 34407–34414.

Manninen, A., Verkade, P., Le Lay, S., Torkko, J., Kasper, M., Fullekrug, J., and Simons, K. (2005). Caveolin-1 is not essential for biosynthetic apical membrane transport. Mol. Cell Biol. *25*, 10087–10096.

Martens, J. R., Sakamoto, N., Sullivan, S. A., Grobaski, T. D., and Tamkun, M. M. (2001). Isoform-specific localization of voltage-gated K+ channels to distinct lipid raft populations. Targeting of Kv1.5 to caveolae. J. Biol. Chem. *276*, 8409–8414.

Martin, P. E., and Evans, W. H. (2004). Incorporation of connexins into plasma membranes and gap junctions. Cardiovasc. Res. *62*, 378–387.

Masgrau-Peya, E., Salomon, D., Saurat, J. H., and Meda, P. (1997). In vivo modulation of connexins 43 and 26 of human epidermis by topical retinoic acid treatment. J. Histochem. Cytochem. *45*, 1207–1215.

Mograbi, B., Corcelle, E., Defamie, N., Samson, M., Nebout, M., Segretain, D., Fenichel, P., and Pointis, G. (2003). Aberrant Connexin 43 endocytosis by the carcinogen lindane involves activation of the ERK/mitogen-activated protein kinase pathway. Carcinogenesis *24*, 1415–1423.

Musil, L. S., and Goodenough, D. A. (1991). Biochemical analysis of connexin43 intracellular transport, phosphorylation, and assembly into gap junctional plaques. J. Cell Biol. *115*, 1357–1374.

Musil, L. S., and Goodenough, D. A. (1993). Multisubunit assembly of an integral plasma membrane channel protein, gap junction connexin43, occurs after exit from the ER. Cell *74*, 1065–1077.

Nichols, B. J. (2002). A distinct class of endosome mediates clathrin-independent endocytosis to the Golgi complex. Nat. Cell Biol. *4*, 374–378.

Ostrom, R. S., and Insel, P. A. (2006). Methods for the study of signaling molecules in membrane lipid rafts and caveolae. Methods Mol. Biol. *332*, 181–191.

Parolini, I. *et al*. (1999). Expression of caveolin-1 is required for the transport of caveolin-2 to the plasma membrane. Retention of caveolin-2 at the level of the Golgi complex. J. Biol. Chem. *274*, 25718–25725.

Parton, R. G., Hanzal-Bayer, M., and Hancock, J. F. (2006). Biogenesis of caveolae: a structural model for caveolin-induced domain formation. J. Cell Sci. *119*, 787–796.

Parton, R. G., and Simons, K. (2007). The multiple faces of caveolae. Nat. Rev. Mol. Cell Biol. *8*, 185–194.

Paznekas, W. A. *et al*. (2003). Connexin 43 (GJA1) mutations cause the pleiotropic phenotype of oculodentodigital dysplasia. Am. J. Hum. Genet. *72*, 408–418.

Pol, A., Martin, S., Fernandez, M. A., Ferguson, C., Carozzi, A., Luetterforst, R., Enrich, C., and Parton, R. G. (2004). Dynamic and regulated association of caveolin with lipid bodies: modulation of lipid body motility and function by a dominant negative mutant. Mol. Biol. Cell *15*, 99–110.

Pol, A., Martin, S., Fernandez, M. A., Ingelmo-Torres, M., Ferguson, C., Enrich, C., and Parton, R. G. (2005). Cholesterol and fatty acids regulate dynamic caveolin trafficking through the Golgi complex and between the cell surface and lipid bodies. Mol. Biol. Cell *16*, 2091–2105.

Qin, H., Shao, Q., Curtis, H., Galipeau, J., Belliveau, D. J., Wang, T., Alaoui-Jamali, M. A., and Laird, D. W. (2002). Retroviral delivery of connexin genes to human breast tumor cells inhibits in vivo tumor growth by a mechanism that is independent of significant gap junctional intercellular communication. J. Biol. Chem. *277*, 29132–29138.

Ray, W. J., Yao, M., Mumm, J., Schroeter, E. H., Saftig, P., Wolfe, M., Selkoe, D. J., Kopan, R., and Goate, A. M. (1999). Cell surface presenilin-1 participates in the γ-secretase-like proteolysis of Notch. J. Biol. Chem. *274*, 36801–36807.

Razani, B. *et al*. (2001). Caveolin-1 null mice are viable but show evidence of hyperproliferative and vascular abnormalities. J. Biol. Chem. *276*, 38121–38138.

Remillard, C. V., and Yuan, J. X. (2006). Transient receptor potential channels and caveolin-1, good friends in tight spaces. Mol. Pharmacol. *70*, 1151–1154.

Roscoe, W., Veitch, G. I., Gong, X. Q., Pellegrino, E., Bai, D., McLachlan, E., Shao, Q., Kidder, G. M., and Laird, D. W. (2005). Oculodentodigital dysplasia-causing connexin43 mutants are non-functional and exhibit dominant effects on wild-type connexin43. J. Biol. Chem. *280*, 11458–11466.

Saez, J. C., Berthoud, V. M., Branes, M. C., Martinez, A. D., and Beyer, E. C. (2003). Plasma membrane channels formed by connexins: their regulation and functions. Physiol. Rev. *83*, 1359–1400.

Sando, G. N., Zhu, H., Weis, J. M., Richman, J. T., Wertz, P. W., and Madison, K. C. (2003). Caveolin expression and localization in human keratinocytes suggest a role in lamellar granule biogenesis. J. Invest. Dermatol. *120*, 531–541.

Sargiacomo, M., Sudol, M., Tang, Z., and Lisanti, M. P. (1993). Signal transducing molecules and glycosyl-phosphatidylinositol-linked proteins form a caveolin-rich insoluble complex in MDCK cells. J. Cell Biol. *122*, 789–807.

Scheiffele, P., Verkade, P., Fra, A. M., Virta, H., Simons, K., and Ikonen, E. (1998). Caveolin-1 and -2 in the exocytic pathway of MDCK cells. J. Cell Biol. *140*, 795–806.

Scherer, P. E., Lewis, R. Y., Volonte, D., Engelman, J. A., Galbiati, F., Couet, J., Kohtz, D. S., van Donselaar, E., Peters, P., and Lisanti, M. P. (1997). Cell-type and tissue-specific expression of caveolin-2. Caveolins 1 and 2 co-localize and form a stable hetero-oligomeric complex in vivo. J. Biol. Chem. *272*, 29337–29346.

Scherer, P. E., Lisanti, M. P., Baldini, G., Sargiacomo, M., Mastick, C. C., and Lodish, H. F. (1994). Induction of caveolin during adipogenesis and association of GLUT4 with caveolin-rich vesicles. J. Cell Biol. *127*, 1233–1243.

Scherer, P. E., Okamoto, T., Chun, M., Nishimoto, I., Lodish, H. F., and Lisanti, M. P. (1996). Identification, sequence, and expression of caveolin-2 defines a caveolin gene family. Proc. Natl. Acad. Sci. USA *93*, 131–135.

Schlegel, A., and Lisanti, M. P. (2000). A molecular dissection of caveolin-1 membrane attachment and oligomerization. Two separate regions of the caveolin-1 C-terminal domain mediate membrane binding and oligomer/oligomer interactions in vivo. J. Biol. Chem. *275*, 21605–21617.

Schlegel, A., Pestell, R. G., and Lisanti, M. P. (2000). Caveolins in cholesterol trafficking and signal transduction: implications for human disease. Front Biosci. *5*, D929–D937.

Schubert, A. L., Schubert, W., Spray, D. C., and Lisanti, M. P. (2002). Connexin family members target to lipid raft domains and interact with caveolin-1. Biochemistry *41*, 5754–5764.

Segretain, D., and Falk, M. M. (2004). Regulation of connexin biosynthesis, assembly, gap junction formation, and removal. Biochim. Biophys. Acta *1662*, 3–21.

Shao, Q., Wang, H., McLachlan, E., Veitch, G. I., and Laird, D. W. (2005). Down-regulation of Cx43 by retroviral delivery of small interfering RNA promotes an aggressive breast cancer cell phenotype. Cancer Res. *65*, 2705–2711.

Shaw, R. M., Fay, A. J., Puthenveedu, M. A., von Zastrow, M., Jan, Y. N., and Jan, L. Y. (2007). Microtubule plus-end-tracking proteins target gap junctions directly from the cell interior to adherens junctions. Cell *128*, 547–560.

Shin, J. L., Solan, J. L., and Lampe, P. D. (2001). The regulatory role of the C-terminal domain of connexin43. Cell Commun. Adhes. *8*, 271–275.

Simons, K., and Ehehalt, R. (2002). Cholesterol, lipid rafts, and disease. J. Clin. Invest. *110*, 597–603.

Singh, D., Solan, J. L., Taffet, S. M., Javier, R., and Lampe, P. D. (2005). Connexin 43 interacts with zona occludens-1 and -2 proteins in a cell cycle stage-specific manner. J. Biol. Chem. *280*, 30416–30421.

Sohl, G., and Willecke, K. (2004). Gap junctions and the connexin protein family. Cardiovasc. Res. *62*, 228–232.

Solan, J. L., and Lampe, P. D. (2005). Connexin phosphorylation as a regulatory event linked to gap junction channel assembly. Biochim. Biophys. Acta *1711*, 154–163.

Song, K. S., Tang, Z., Li, S., and Lisanti, M. P. (1997). Mutational analysis of the properties of caveolin-1. A novel role for the C-terminal domain in mediating homo-typic caveolin-caveolin interactions. J. Biol. Chem. *272*, 4398–4403.

Tada, J., and Hashimoto, K. (1997). Ultrastructural localization of gap junction protein connexin 43 in normal human skin, basal cell carcinoma, and squamous cell carcinoma. J. Cutan. Pathol. *24*, 628–635.

Tagawa, A., Mezzacasa, A., Hayer, A., Longatti, A., Pelkmans, L., and Helenius, A. (2005). Assembly and trafficking of caveolar domains in the cell: caveolae as stable, cargo-triggered, vesicular transporters. J. Cell Biol. *170*, 769–779.

Thomas, T., Jordan, K., Simek, J., Shao, Q., Jedeszko, C., Walton, P., and Laird, D. W. (2005). Mechanisms of Cx43 and Cx26 transport to the plasma membrane and gap junction regeneration. J. Cell Sci. *118*, 4451–4462.

Toselli, M., Biella, G., Taglietti, V., Cazzaniga, E., and Parenti, M. (2005). Caveolin-1 expression and membrane cholesterol content modulate N-type calcium channel activity in NG108–15 cells. Biophys. J. *89*, 2443–2457.

Toyofuku, T., Yabuki, M., Otsu, K., Kuzuya, T., Hori, M., and Tada, M. (1998). Direct association of the gap junction protein connexin-43 with ZO-1 in cardiac myocytes. J. Biol. Chem. *273*, 12725–12731.

Trouet, D., Hermans, D., Droogmans, G., Nilius, B., and Eggermont, J. (2001). Inhibition of volume-regulated anion channels by dominant-negative caveolin-1. Biochem. Biophys. Res. Commun. *284*, 461–465.

Trouet, D., Nilius, B., Jacobs, A., Remacle, C., Droogmans, G., and Eggermont, J. (1999). Caveolin-1 modulates the activity of the volume-regulated chloride channel. J. Physiol. *520*, 113–119.

van Steensel, M. A., Spruijt, L., van der Burgt, I., Bladergroen, R. S., Vermeer, M., Steijlen, P. M., and van Geel, M. (2005). A 2-bp deletion in the GJA1 gene is associated with oculo-dento-digital dysplasia with palmoplantar keratoderma. Am. J. Med. Genet. A. *132*, 171–174.

Vreeburg, M., de Zwart-Storm, E. A., Schouten, M. I., Nellen, R. G., Marcus-Soekarman, D., Devies, M., van Geel, M., and van Steensel, M. A. (2007). Skin changes in oculo-dento-digital dysplasia are correlated with C-terminal truncations of connexin 43. Am. J. Med. Genet. A. *143*, 360–363.

Wang, X. L., Ye, D., Peterson, T. E., Cao, S., Shah, V. H., Katusic, Z. S., Sieck, G. C., and Lee, H. C. (2005). Caveolae targeting and regulation of large

conductance Ca(2+)-activated K+ channels in vascular endothelial cells. J. Biol. Chem. *280*, 11656–11664.

Wei, C. J., Xu, X., and Lo, C. W. (2004). Connexins and cell signaling in development and disease. Annu. Rev. Cell Dev. Biol. *20*, 811–838.

Williams, T. M., and Lisanti, M. P. (2004). The caveolin proteins. Genome Biol. *5*, 214.

Wyse, B. D., Prior, I. A., Qian, H., Morrow, I. C., Nixon, S., Muncke, C., Kurzchalia, T. V., Thomas, W. G., Parton, R. G., and Hancock, J. F. (2003). Caveolin interacts with the angiotensin II type 1 receptor during exocytic transport but not at the plasma membrane. J. Biol. Chem. *278*, 23738–23746.

Yarbrough, T. L., Lu, T., Lee, H. C., and Shibata, E. F. (2002). Localization of cardiac sodium channels in caveolin-rich membrane domains: regulation of sodium current amplitude. Circ. Res. *90*, 443–449.